*Bulletin of the New Zealand Society for Earthquake Engineering, Vol. 58, No. 1, March 2025*

# SITE CLASSIFICATION METHODOLOGY FOR TS 1170.5 DESIGN SPECTRA

**Robin L. Lee[1], Misko Cubrinovski[2] and Brendon A. Bradley[3]**

(Submitted *March 2024*; Reviewed *May 2024*; Accepted *January 2025*)


## ABSTRACT

The Technical Specification (TS) 1170.5 has been developed to incorporate the output of the 2022 New Zealand National Seismic Hazard Model revision (NSHM2022) [1] and update Clause B1 Verification Method 1 (B1/VM1) of the New Zealand Building Code. In this paper, we discuss the proposed site classification methodology based on $V_{s(30)}$ (i.e., the time-averaged shear-wave velocity from the ground surface to 30 m depth) which is used to incorporate site effects in the TS 1170.5 design spectra. The reasoning for the use of $V_{s(30)}$ for site classification, a significant departure from New Zealand Standards NZS 1170.5 [2], is first elaborated. Based on detailed scrutiny of uniform hazard spectra obtained from NSHM2022, seven site classes are proposed, with associated design spectra for six of the site classes. Multiple objectives were considered in the definition of TS 1170.5 site classes, with the principal goal being to represent relevant site conditions in a robust yet practical manner, appropriate for engineering design practice. As $V_{s(30)}$ is the principal parameter in the site classification scheme, the establishment of the $V_s$ profile at the site is a critical step. Several methods for obtaining a $V_s$ profile, measured or inferred, and subsequent calculation of $V_{s(30)}$ are recommended. Each method is associated with a different uncertainty factor that affects both site classification and consequent design spectra. In this context, a multiple site class definition must be adopted with an envelope design spectrum in cases where the range of $V_{s(30)}$ values span several site classes. Importantly, the variation in design spectra due to uncertainty in the site class is relatively small compared to the uncertainty in the uniform hazard spectra themselves (due to uncertainties in NSHM2022 and PSHA). For sites with ground conditions not well-represented within the PSHA performed for NSHM2022, site-specific (special) studies are recommended.


https://doi.org/10.5459/bnzsee.1686

## INTRODUCTION

The 2022 New Zealand (NZ) National Seismic Hazard Model revision (NSHM2022) [1] has triggered the need to re-examine the NZ seismic design provisions, NZS 1170.5 [2]. For this purpose, the Seismic Risk Working Group (SRWG) was established to propose updates to Clause B1 Verification Method 1 (B1/VM1) of the NZ Building Code. In the first phase of the SRWG efforts, a Technical Specification (TS) document was developed, TS 1170.5, which is expected to be released in 2025. TS 1170.5 incorporates the output from NSHM2022 and provides a methodology for determination of seismic design loads for buildings. This paper outlines the proposed changes to the site classification scheme and determination of horizontal design actions for different site classes.

In the first part of the paper, the influence of seismic site effects on observed response spectra, and common approaches for their incorporation into design codes are briefly discussed. Details of the proposed site classification scheme in TS 1170.5 are then presented, including justification of the adopted approach and design spectra. Methods for evaluation of shear-wave velocity ($V_s$) profiles, and their use for determination of site class are discussed, including reasoning behind their use and justification of the proposed uncertainty factors for each method. To facilitate the implementation of the proposed methodology, examples for evaluation of site classes are presented in Appendix B for a range of scenarios including various site conditions and available geotechnical data.

## BACKGROUND

### Observations from Recent NZ Earthquakes

The influence of site effects on the ground motion characteristics can be complex and involve various factors, such as soil stiffness (as represented by the $V_s$ of soils), thickness of the soil deposit, ratio of impedance (product of $V_s$ and mass density) between soil layers and with the underlying bedrock, fundamental period of the site, and the effects of nonlinear soil behavior. Figure 1 illustrates typical site effects on the response spectra of ground motions recorded in recent NZ earthquakes. Each plot comparatively shows 5% damped elastic response spectra of records obtained at the ground surface of two nearby sites, one on a nominally rock site, and the other on a soft soil site. Given their small separation distance relative to the earthquake source, the contribution of source and path effects are (practically) identical (e.g., earthquake magnitude, source-to-site distance, orientation of the site relative to the source), and hence the differences between the two spectra in each plot are solely due to site effects.

Figure 1a shows records at two Lyttelton sites which are in proximity to each other, just several hundred metres apart. The sites are close to the source (approximately 2 km source-to-site distance) of the 2011 Christchurch ($M_w$6.2) earthquake. Due to the short distance from the source, the record on rock (LPCC) is characterized by high spectral accelerations ($S_a$) of 2-3 g over short periods ($T$ < 0.3 s), and a high peak ground acceleration ($PGA$) of 0.8 g. The spectral accelerations markedly reduce over periods of 0.3 s to 1.0 s, and remain low $S_a \leq 0.2$ g for $T >$

[1] *Corresponding Author, Senior Lecturer, University of Canterbury, Christchurch, robin.lee@canterbury.ac.nz (Member)*
[2] *Professor, University of Canterbury, Christchurch (Member)*
[3] *Professor, University of Canterbury, Christchurch (Member)*

1.0 s. At the nearby soft soil site (LPOC), the response spectra show markedly different characteristics. The extremely high shaking intensity at the bedrock level caused significant nonlinearity in the response of the soft soils (i.e., degradation in stiffness, large shear strains, and a substantial increase of damping in soils). Consequently, a large reduction of spectral accelerations (including *PGA*) is seen at short periods (i.e., loss of high-frequency content). Conversely, appreciable amplification of spectral accelerations (relative to the rock motion) is evident for longer periods from 1-2 seconds due to the response of soft soils.

Figure 1b shows equivalent plots for two Wellington sites, which are also close to each other (approximately 1 km apart), but at a large distance (approximately 60 km) from the source of the 2016 Kaikōura ($M_w$7.8) earthquake. Given the large source-to-site distance, the rock ground motion (POTS) shows low spectral accelerations across all periods including a low $PGA \approx 0.08$ g. It is evident, however, that the soft soil site (CPLB) significantly amplifies the spectral amplitudes across all periods, and especially in the period range between 1.5 to 2.0 s. The two sets of response spectra shown in Figure 1 clearly demonstrate profound site effects on the ground motion characteristics including the strong influence of such effects on the intensity of ground shaking.

### Site Effects in Design Codes

The important influence of site conditions on response spectra has been recognized soon after the introduction of the response spectrum concept [3,4] and formalisation of the standard (average) shape of response spectra [5]. Hayashi et al. [6] have shown that the average normalized acceleration response spectra of ground motions recorded in Japan had distinctly different characteristics for three types of sites (i.e., very dense soils, intermediate soils, and very loose soils). Similarly, Seed et al. [7], using ground motion records from California, USA, showed clear differences in the average acceleration response spectra for different soil and geological conditions, and indicated the need to consider site effects in the seismic design of structures. The rapid accumulation of ground motion records over the past several decades have confirmed these general trends and provided additional evidence for the complex site effects on response spectra.

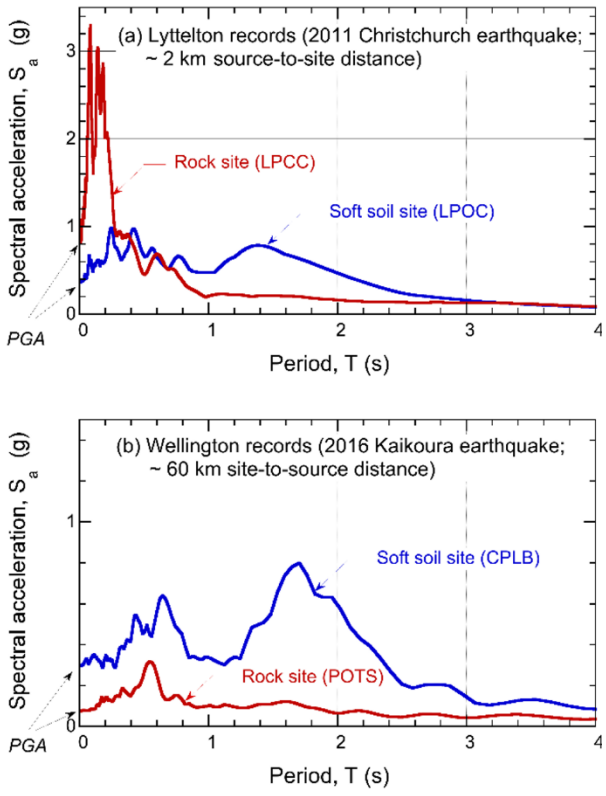


***Figure 1: Illustration of significant site effects on response spectra observed in recent New Zealand earthquakes: (a) near-fault records of 2011 Christchurch earthquake (approx. 2 km from the source) at two nearby sites in Lyttelton, one on rock (red line) and the other on soft soil site (blue line); (b) far-field records of 2016 Kaikōura earthquake at two nearby sites in Wellington (approx. 60 km from the source), one on rock (red line) and the other on soft soil site of reclaimed land (blue line).***

In modern design codes, seismic design actions for buildings are generally defined in the form of design spectra, which are derived from probabilistic seismic hazard analysis (PSHA). For any given location, it is common for 5% damped elastic pseudo-acceleration design spectra to be defined for several site classes (e.g., hard rock, rock, stiff soil, soft soil, and very soft soils). The site classification is essentially based on the types of soils and their properties, with the intention to quantify the overall differences in the response spectra of different site classes, in a general (i.e., average) sense.

Design codes aim to account for site effects in a manner that is sufficiently accurate for engineering design and is easy to apply in practice (i.e., balancing uncertainty, level of effort and relevance for design). To achieve these goals, site classification schemes typically involve the following considerations: (i) the most typically encountered ground conditions are organized into several specific categories (site classes), so that each site class is characterized by a distinct set of design spectra; (ii) the design objectives should be achieved using a practical (i.e., small) number of discrete site classes; and, (iii) site classification should be based on a small number of soil/site parameters that are easy to implement in practice.

Figure 2a and 2b show characteristic design spectra for different soil classes presented in ASCE 7-22 [8] for a site in Downtown Los Angeles and NZS 1170.5 [2] for a site in Wellington, respectively. Each set of spectra show the characteristic trend in which softer soil sites are characterised by a wider spectral plateau (i.e., constant acceleration branch) and higher spectral accelerations over medium to long periods (i.e., accelerations for post-corner periods). They clearly illustrate the significant influence of site conditions on the acceleration spectra in design codes.

One important difference between the design spectra presented in ASCE 7-22 (Figure 2a) and NZS 1170.5 (Figure 2b) is in the parameters used for site classification. ASCE 7-22 uses $V_{s(30)}$ (time-averaged shear wave velocity to 30 m depth; also commonly referred to in the literature as $V_{s30}$) to determine site classes, whereas NZS 1170.5 uses a combination of geotechnical parameters (e.g., SPT resistance, undrained shear strength) and maximum depth of soils to identify site classes.

### Site Effects in PSHA

PSHA is the underlying methodology for the development of elastic site spectra in seismic loading standards. It essentially involves three principal steps: (i) characterisation of earthquake sources; (ii) estimation of ground shaking intensity for each source realisation (rupture); and (iii) summation/integration of the effects of steps (i) and (ii) over all relevant earthquake sources for a given site (e.g. Baker et al. [9]). In particular, ground motion intensity measures (IMs) are conventionally predicted using ground motion models (GMMs) which are based on previously observed ground motion data and additional considerations from theory and numerical simulation. In general, GMMs are functions of source, path and site parameters. Examples of typical parameters used in GMMs

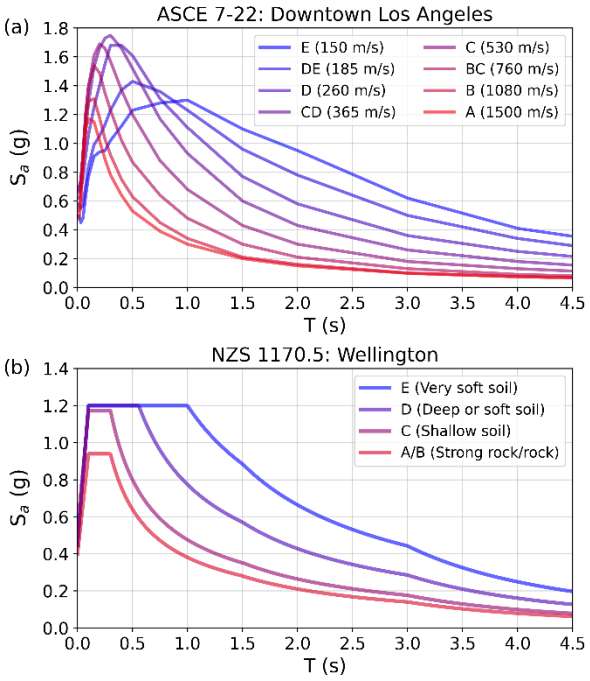


***Figure 2: Design spectra illustrating the effect of site class for: (a) Downtown Los Angeles multi-period design spectra based on ASCE 7-22; and (b) Wellington based on NZS 1170.5. ASCE 7-22 provides design spectra up to 10 s period but is only plotted here to 4.5 s for parity with the NZS 1170.5 design spectra.***

include moment magnitude and faulting style (source parameters), source-to-site distances (path parameters), and $V_{s(30)}$, $Z_{1.0}$ and $Z_{2.5}$ (depths to $V_s$ = 1.0 km/s and $V_s$ = 2.5 km/s horizons, respectively), as site parameters. For the treatment of site effects, modern GMMs (e.g., NGA-West2 [10] and NGA-Subduction [11]), without exception, all make use of $V_{s(30)}$ as the primary variable to model site effects. These models additionally consider other $V_s$ depth horizons, for example $Z_{1.0}$ and $Z_{2.5}$, to attempt to account for the role of deeper geologic structure on ground motions.

The treatment of site effects in PSHA is critically important for the site classification methodology in any design provision, as it essentially imposes constraints on the site parameter(s) that can be used for site classification in order to remain internally consistent with the underlying PSHA results that the design spectra are based upon. That is, ideally, the parameter(s) used for site classification should be the same as those used for modelling site effects in PSHA. In this context, $V_{s(30)}$ has been commonly adopted as a parameter for site classification in seismic codes (e.g., BSCC [12]; EN1998-1 [13]; NBCC [14]; ASCE7-16 [15]; ASCE7-22 [8]). $V_{s(30)}$ is certainly not a perfect predictor of site effects, however, to date, no better performing alternative has been widely adopted internationally for evaluation of site effects within PSHA.

## PSHA WITHIN NSHM2022

NSHM2022 represents a significant advancement in the treatment of seismic hazard in NZ relative to the preceding study [16] which underpinned NZS 1170.5 [2]. Gerstenberger et al. [1] provide a summary of these advances and references to specific documentation. With regard to the treatment of seismic site effects, in particular, all adopted ground motion models consider the salient phenomena (impedance-based amplification, reflection, refraction, etc.) through scaling with $V_{s(30)}$ and $Z_{1.0}$ or $Z_{2.5}$ parameters. Generally speaking, these effects are decomposed into linear and nonlinear scaling functions. The linear component exhibits an increase in ground motion intensity with reducing $V_{s(30)}$ values, with a functional form based on some theoretical considerations, but principally constrained using significant observational data. The nonlinear component accounts for any amplitude-dependent deamplification that is a function of site parameters as well as the intensity of the ground motion at the site (for a reference site condition). Owing to the general paucity of high-intensity observed ground motions for soft soil sites, numerical simulations are used to supplement observational data in the development and calibration of the nonlinear component of these site response models. The site response models used within the PSHA for NSHM2022 were the default site effect terms included in each GMM. Bradley et al. [17] provides further detail on the adopted GMMs considered in NSHM2022.

In the PSHA performed within NSHM2022, $V_{s(30)}$ has been used as the only explicitly-defined parameter for the effects of site conditions on ground motion characteristics. Other site parameters, such as $Z_{1.0}$ or $Z_{2.5}$ were considered not to be routinely available for all possible locations of practical application in NZ, and thus the effects of deeper velocity structure on ground motions are only implicitly considered through the inherent correlation between $V_{s(30)}$ and $Z_{1.0}$ or $Z_{2.5}$ (e.g., Abrahamson et al. [18] and Chiou and Youngs [19]). NSHM2022 directly provides uniform hazard spectra for $V_{s(30)}$ values over the range of $V_{s(30)}$ = 150 m/s to 1500 m/s. Thus, $V_{s(30)}$ is the only parameter for ground conditions that can directly link the derived NSHM2022 response spectra (and hence uniform hazard spectra) to site characteristics, and therefore is the obvious choice as a parameter for site classification.

### Effects of $V_{s(30)}$ on Uniform Hazard Spectra

The effects of $V_{s(30)}$ on uniform hazard spectra resulting from the NSHM2022 were examined for a number of test locations across NZ. Figure 3 shows uniform hazard spectra for Auckland, Christchurch and Wellington, for annual probability of exceedances (APoE) 1/25, 1/500, and 1/2500. Each plot shows acceleration spectra for six values of $V_{s(30)}$ in the range between 175 m/s and 750 m/s, that are the adopted characteristic $V_{s(30)}$ values for each of the TS 1170.5 site classes, as discussed subsequently.

It is important to recognize the variable shaking intensities associated with each plot in Figure 3, as the shape of spectra for a given $V_{s(30)}$ is strongly affected by the shaking intensity. At low shaking intensities (e.g., Figure 3a; APoE 1/25 for Auckland), spectral accelerations increase as $V_{s(30)}$ reduces, as softer soils amplify the response across all periods. Conversely, at very high shaking intensity (e.g., Figure 3i; APoE 1/2500 for Wellington), softer soils exhibit highly nonlinear response which reduces spectral accelerations at short periods (relative to stiffer soils and rock), but still amplify spectral accelerations at moderate-to-long periods. Spectral characteristics for intermediate shaking intensities gradually transition between the spectral shapes typical for low and high shaking intensities.

It is worth noting that the effects of soft soils on the uniform hazard spectra depicted in Figure 3a and 3i, are equivalent to those shown in Figure 1b and 1a, respectively. While Figure 1 illustrates effects of site conditions on acceleration response spectra for two specific earthquake events and set of records, Figure 3 depicts how such effects are represented, in an average sense, in uniform hazard spectra obtained from PSHA.

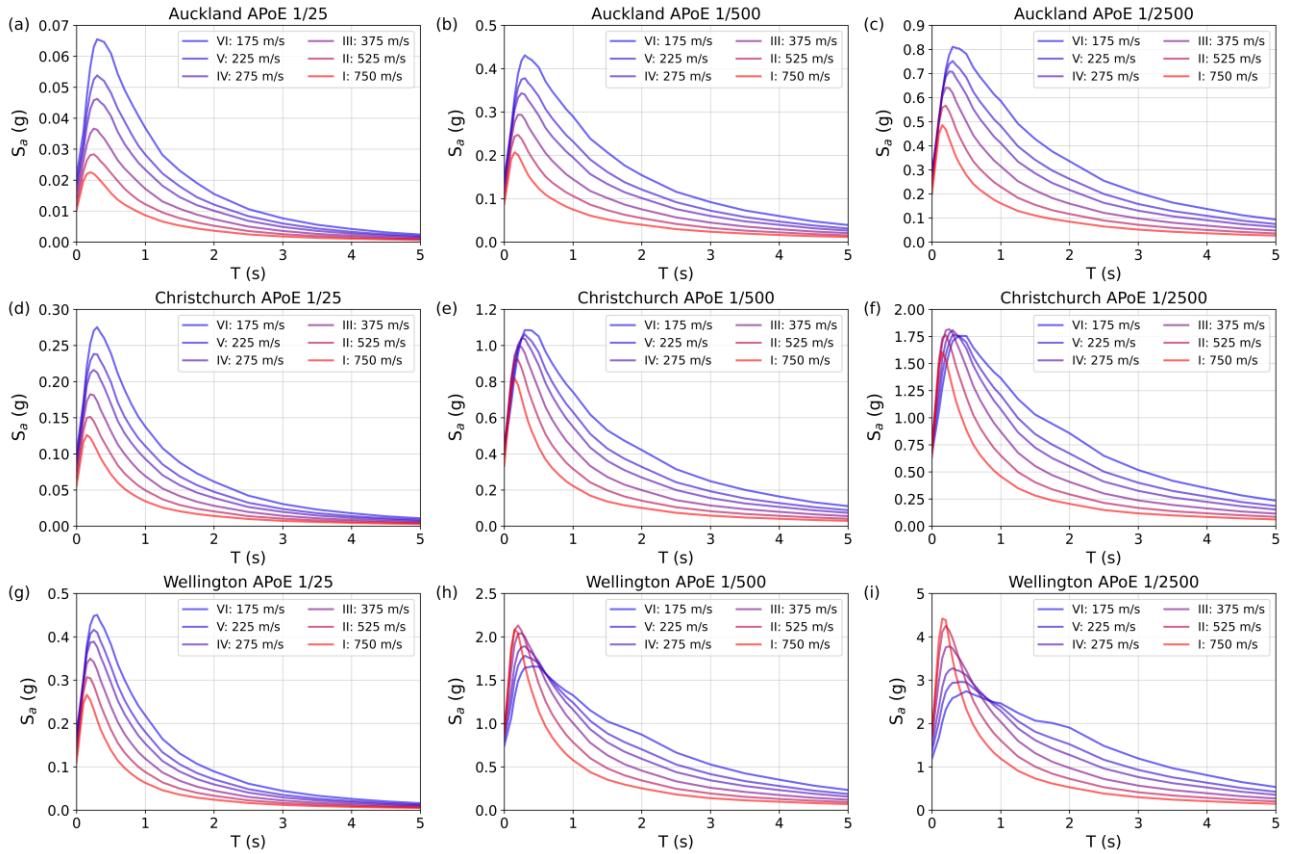


***Figure 3: Uniform hazard spectra from NSHM2022 for characteristic $V_{s(30)}$ values at three annual probability of exceedances 1/25, 1/500 and 1/2500, in Auckland, Christchurch and Wellington. Each subfigure has a different vertical scale.***

## PROPOSED SITE CLASSIFICATION

Based on a comprehensive scrutiny of the uniform hazard spectra derived from NSHM2022, a site classification scheme was developed in which $V_{s(30)}$ was used as the principal site characterisation parameter. The site classes proposed in the TS 1170.5 are summarised in Table 1. It should be emphasized that the site classification is based on $V_{s(30)}$ and some additional criteria which aims to either address specific site conditions for which $V_{s(30)}$ alone is insufficient to identify the site class or to facilitate site classification in practice. Thus, conventional geotechnical parameters such as undrained shear strength of soils, standard penetration test (SPT) resistance of soils ($N_{60}$), and cone penetration test (CPT) tip resistance ($q_c$) are used to facilitate characterisation of soft soils and discriminating between Site Classes V and VI. Similarly, the presence of soil or highly-weathered rock has been used to discriminate between Site Classes I and II. The additional criteria (provided in Table 3.1 of TS 1170.5 and reproduced here in Table A1 in Appendix A) are used in conjunction with the $V_{s(30)}$-based criteria.

Using the uniform hazard spectra from NSHM2022 for the characteristic $V_{s(30)}$ values (shown in brackets in Table 1), design acceleration response spectra for Site Classes I to VI were developed based on the methodology presented in Francis et al. [20]. As an example, Figure 4 shows the proposed design spectra for Site Classes I to VI, for three APoE 1/25, 1/500 and 1/2500, for Auckland, Christchurch and Wellington (TS 1170.5). Note that Auckland design spectra are based on 90$^{th}$ percentile uniform hazard spectra rather than the mean uniform hazard spectra that are shown in Figure 3. The methodology for determination of site class, which is clearly the critical step in the determination of the design spectra for the site, is discussed in the following section.

***Table 1: Proposed site classes in TS 1170.5. The $V_{s(30)}$ ranges provided are for determination of which site class a given site resides in.***

| Site Class | Description | $V_{s(30)}$ (m/s) |
|---|---|---|
| I | Rock site | > 750 (750)* |
| II | Very stiff soil, very dense soil or soft rock | 450 – 750 (525)* |
| III | Stiff or dense soil | 300 – 450 (375)* |
| IV | Moderately stiff or medium dense soil | 250 – 300 (275)* |
| V | Soft or loose soil | 200 – 250 (225)* |
| VI | Very soft or very loose soil | 150 – 200 (175)* |
| VII | Very soft or very loose soil (requiring special considerations) | ≤ 150 |

** The $V_{s(30)}$ values in brackets are the characteristic value associated with uniform hazard spectra from NSHM2022 that the design spectra are derived from.*

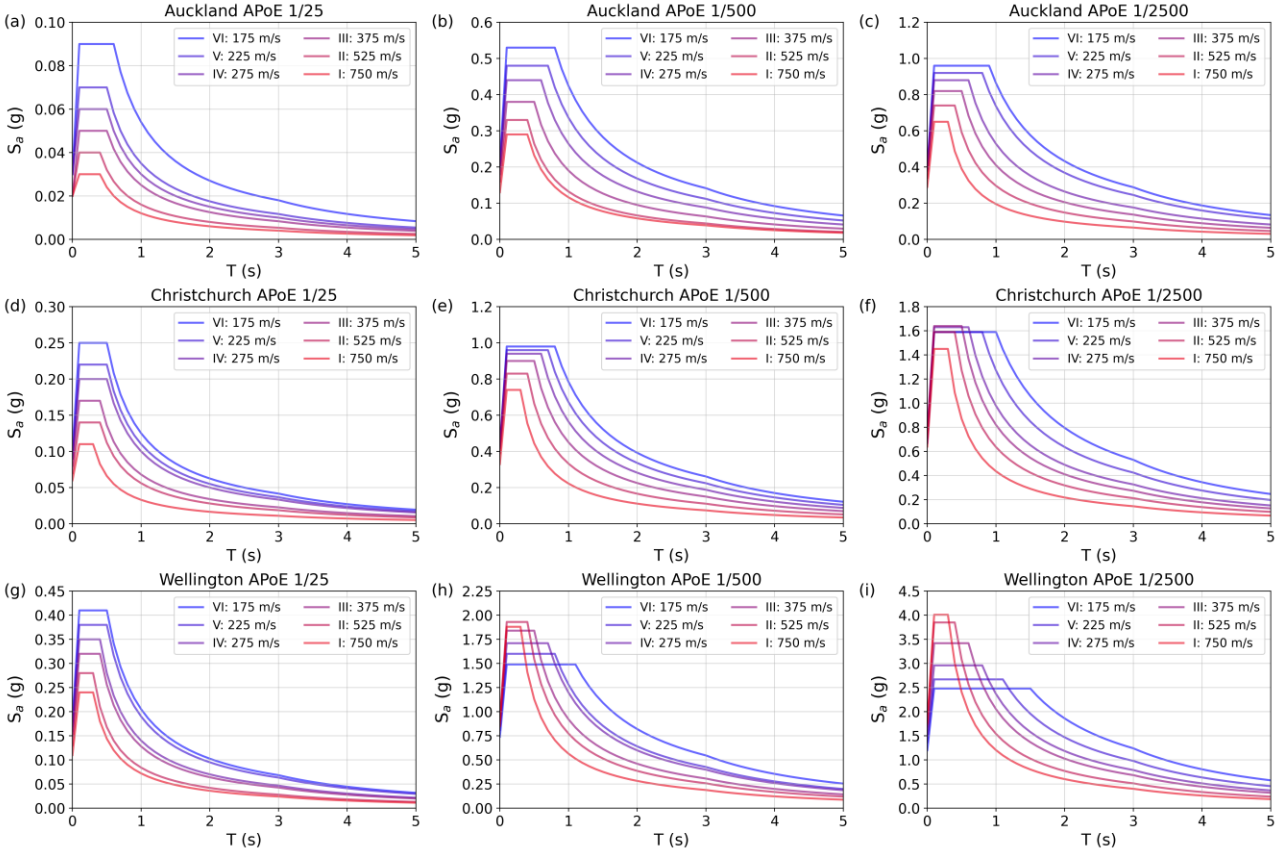


***Figure 4: Design spectra from TS 1170.5 for all site classes at three annual probability of exceedances 1/25, 1/500 and 1/2500, in Auckland, Christchurch and Wellington. Each subfigure has a different vertical scale.***

The $V_{s(30)}$ ranges for the site classes (as well as the characteristic $V_{s(30)}$ values shown in brackets in Table 1) were defined based on the following three criteria: (i) to represent the most typically encountered site conditions relevant for engineering design; (ii) to provide greater granularity in spectral characteristics for the most commonly encountered site conditions in populated regions across New Zealand (i.e., $V_{s(30)}$ between 200 m/s and 300 m/s; Kaiser et al. [21], Wotherspoon et al. [22]; NZ Geotechnical Database; and insights from Foster et al. [23] and Perrin et al. [24]); and (iii) to achieve reasonably uniform increments of spectral values between site classes that satisfy the trade-off requirements between practicality (small number of site classes) and accuracy required for a coherent design. To illustrate the last point, Figure 5 shows the mean spectral ratios of adjacent site classes for the TS 1170.5 design spectra computed for 12 different locations corresponding to a variety of significant population centres across NZ (Auckland, Tauranga, Gisborne, Napier, Masterton, Wellington, Nelson, Blenheim, Greymouth, Christchurch, Queenstown, Dunedin). The figure shows that spectral accelerations of adjacent site classes are generally within 20-40% from each other, and that lower spectral increments (approximately 20-25%) have been achieved for the most commonly encountered site conditions in populated regions (i.e., for $V_{s(30)}$ between 200 m/s and 300 m/s). The ±1 standard deviation of the spectral ratios between site classes II/I and VI/V (shown by the shaded areas) are included to illustrate the variation between the 12 locations. With the exception of the spectral ratio between site classes II/I for APoE 1/25, the standard deviations are typically less than approximately 0.1, indicating that these ratios have relatively low variation across the country. Note that for APoE 1/25 the values of spectral accelerations are low, and hence, even a high percentage difference in spectral ratios actually implies a small change in spectral accelerations.

### Sites Requiring Special Considerations

Site Classes VI and VII are used for very soft or very loose soils. They generally have very similar characteristics except for the difference in their $V_{s(30)}$ value, with Site Class VII soils having the lowest $V_{s(30)} \leq 150$ m/s. As sites with $V_{s(30)} \leq 150$ m/s are

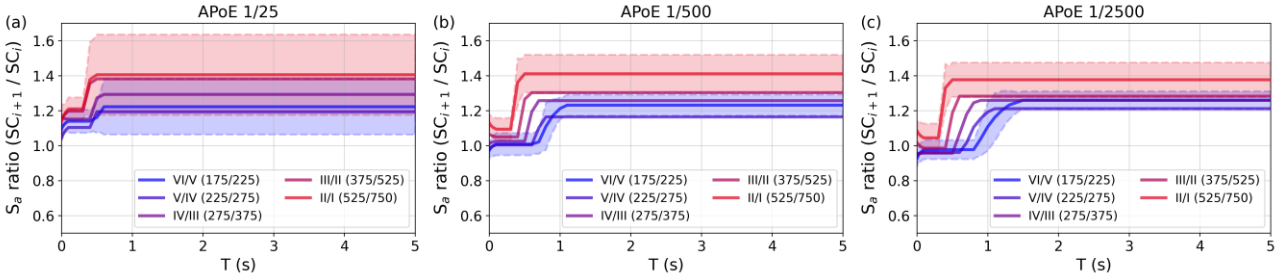


***Figure 5: Mean spectral ratios for adjacent TS 1170.5 site classes across 12 locations for: (a) APoE 1/25; (b) APoE 1/500; and (c) APoE 1/2500. Shaded areas correspond to ±1 standard deviation of the spectral ratios for site classes II/I in red and VI/V in blue.***

generally not well represented in the empirical database of recorded ground motions, empirical GMMs used in the NSHM2022 are less well constrained for predicting ground motions for such sites. Therefore, design spectra for Site Class VII soils are not presented in TS 1170.5. Instead, Site Class VII soils require site-specific study in which the dynamic behaviour of soils and their effects on ground motion characteristics and response spectra will be rigorously considered (details of which are provided in Section C3.1.3.2 of TS 1170.5). Large ground deformation and ground failure, including effects of liquefaction (pore water pressure generation and strength loss) are likely at such sites and should be subjected to separate scrutiny and additional analyses. Guidance on effects of liquefaction on land and structures can be found in NZGS/MBIE Module 3 [25] and earthquake-resistant design of foundations can be found in NZGS/MBIE Module 4 [26].

### Default Design Spectra

It is generally expected that appropriate site investigations will be needed for geotechnical characterisation of the foundation soils, for reasons other than site classification for design spectra. This would include considerations in relation to seismic behaviour of foundations, soil liquefaction, effects of large ground deformation and soil instability. Provided that such issues have been addressed through an appropriate engineering evaluation, and geotechnical and geologic data confirm that Site Class VI or VII soils are not present at the site, a Default Site Class can be adopted for the site, which is an envelope of the design spectra for Site Classes II, III, IV and V. In practice, this may occur in regions/areas where the geology is well known, and existing nearby site investigations and more limited site investigations typical of other geotechnical design aspects may be sufficient to confirm with confidence that soils that are characteristic of Site Classes VI and VII are not present. Figure 6 shows examples of default spectra typical for low (Figure 6a) and high intensity shaking (Figure 6b) cases. Clearly, the default design spectra employ a conservative estimate of design loads due to the inability to reasonably estimate the site class. Furthermore, for Importance Level 1 and 2 structures, TS 1170.5 permits to adopt the maximum of the short-period spectral accelerations for Site Classes II, III, IV, V and VI

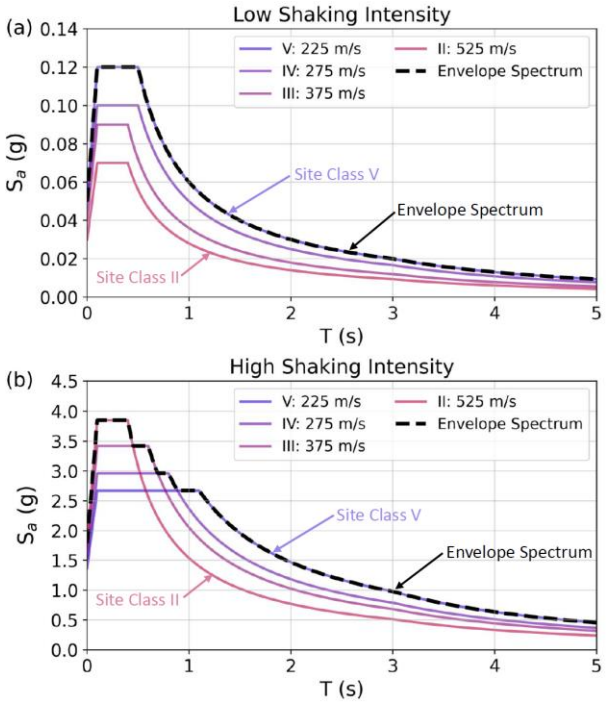


***Figure 6: Examples of default site class envelopes for: (a) low shaking intensity; and (b) high shaking intensity.***

across all periods, without the need to confirm that Site Class VI or VII soils are not present at the site, provided that the impact of deformations in the foundation soils will be addressed through appropriate geotechnical assessment.

## METHODOLOGY FOR DETERMINATION OF SITE CLASS

A detailed step-by-step procedure for classifying a site is provided in the TS 1170.5 Commentary (Section C3.1.3.1 of TS 1170.5). Each step in the procedure is important and aims collectively to provide a coherent and practical way of identifying an appropriate site class and design spectra for the site of interest. As $V_{s(30)}$ is the principal parameter in the site classification scheme, the establishment of the $V_s$ profile at the site is the critical step. In this section, the proposed methods for evaluation of the $V_s$ profile and estimating $V_{s(30)}$ are presented and discussed. To facilitate the interpretation and implementation of each method in practical applications, several examples of $V_{s(30)}$ calculation and site class determination for some typical scenarios are presented in Appendix B.

Three methods for evaluation of $V_s$ profiles at a site have been deemed appropriate for site class determination:

- Method 1: Based on direct field measurement of $V_s$ over the 'full' profile at the site.
- Method 2: Based on direct field measurement of $V_s$ to a depth of at least 15 m at the site.
- Method 3: Based on inferred $V_s$ from correlations using CPT or SPT measurements, or a combination of such penetration measurements and direct field measurements of $V_s$ where the necessary depth requirements of Method 1 and Method 2 are not satisfied.

Each method results in a different level of confidence in the estimated $V_{s(30)}$ for the site, and hence, is associated with a different uncertainty factor in the definition of the site class and design spectra. A range of $V_{s(30)}$ values are needed to account for inherent uncertainties in the measurement of $V_s$, use of empirical correlations, or due to incomplete $V_s$ values (measured and/or inferred) from the ground surface to a depth of 30 m. The following uncertainties in the estimated $V_{s(30)}$ values have been proposed for the three methods:

- Method 1 (Measured $V_s$): 5%
- Method 2 (Partially Measured $V_s$): Linearly interpolated between:
  - 15% for measured $V_s$ to a depth of 15 m, and
  - 5% for measured $V_s$ to a depth of 25 m
- Method 3 (Inferred $V_s$): 30%

The uncertainties associated with each method have been guided by analyses comparing relevant models and data, existing literature, and international design code considerations (e.g., ASCE 7-22 [8]). Method 2 and Method 3 are associated with larger uncertainty than Method 1 because the techniques and models used to estimate $V_s$ for either part of the profile or the entire profile down to 30 m are less accurate than a direct $V_s$ measurement.

It has to be emphasised that general geologic maps (such as QMaps or other surficial geologic maps) are not appropriate for estimating $V_{s(30)}$ as they do not provide the required details for the soil units throughout the depth of the profile. Similarly, national and regional $V_{s(30)}$ maps based on geologic and terrain models (e.g., Foster et al. [23]) are not appropriate for site-specific evaluation of $V_{s(30)}$, and such generic maps are not intended for site-specific engineering assessment.

**Method 1: Evaluation of $V_{s(30)}$ based on Direct Field Measurement of $V_s$ to at least 25 m Depth**

In Method 1, the $V_s$ profile is established from direct $V_s$ field measurements at the site from the ground surface to, ideally, 30 m or greater depth. In cases where the $V_s$ measurement extends to a depth of less than 30 m, but more than 25 m, it is permitted to extend the $V_s$ of the last measured layer to 30 m depth, and proceed with the calculation of $V_{s(30)}$. This relaxation of the depth requirement is justified by the empirical evidence that $V_{s(30)}$ estimates based on $V_s$ data from the ground surface to 25 m depth are typically very similar to (only slightly lower than) $V_{s(30)}$ estimates obtained from $V_s$ data up to 30 m depth.

Measurements of $V_s$ can be obtained either from invasive methods, such as seismic CPT (sCPT), seismic dilatometer (sDMT), downhole or crosshole testing techniques, suspension logging, or using inversion of non-invasive geophysical measurements. Non-invasive geophysical methods include active-source methods (such as Multi-channel Analysis of Surface Waves – MASW), passive-source surface wave methods and S-wave refraction methods. Details on various methods for measurement of $V_s$ profiles are provided in NZGS/MBIE Module 2 [27] and other literature [28-31]. For the direct measurement of $V_s$ (used in Method 1 and Method 2), the key requirement is that high-quality measurements are performed in conjunction with subsequent rigorous treatment and interpretation of data. Given the non-uniqueness of the inversion outcomes in the interpretation of surface wave measurements of $V_s$, it is recommended to use an appropriate number of best-fit profiles that will illustrate the uncertainties in the $V_s$ profiles and $V_{s(30)}$ estimates, including across various parameterisations of the inversions. Subsequently, the average $V_{s(30)}$ across all profiles should be used as the representative $V_{s(30)}$ for the site. Best-fit profiles refer to those with lowest misfit between the associated theoretical dispersion curve(s) and the experimental (observed) dispersion curve(s). It is also recommended that the following details are provided as part of the project documentation: (i) experimental dispersion curves from the surface wave tests; (ii) plots comparing the observed dispersion curves to the theoretical dispersion curves associated with the inverted profiles. Explicit recommendations for reporting surface wave methods are provided here to address the more limited familiarity with these techniques in NZ geotechnical practice, relative to invasive methods, at the time of writing. However, the importance of proper reporting of invasive methods is also acknowledged and comprehensive reporting guidelines for both invasive and non-invasive methods can be found in the NZGS Ground Investigations Specification document [32]. Some methods of $V_s$ measurement can have difficulties in obtaining accurate $V_s$ values at shallow depths, for example due to discrepancies in assumed and real wave travel paths [33]. For such methods (e.g., sCPT, sDMT and downhole techniques), it is recommended that the adopted $V_s$ for $z$ = 0-3 m depth is equal to the average of the measured $V_s$ between $z$ = 2.5-3.5 m, while methods without such issues at shallow depths (e.g., non-invasive surface wave methods) do not require this adjustment.

Uncertainty associated with direct measurement of $V_s$ is difficult to precisely quantify due to limited co-located deep site investigations. Seyhan et al. [34] provides an analysis of the variability between $V_{s(30)}$ determined at 24 sites located in the United States of America and Japan where multiple measured $V_s$ profiles are available for each site, including both surface wave and borehole methods. While the uncertainty in $V_{s(30)}$ differed between sites, it was noted that a reasonable value is $\sigma_{\ln(V_{s(30)})}$ = 0.06 for sites where the geology is relatively uniform across the area. In other words, where rapid variation in $V_{s(30)}$ due to changes in geologic formations or basin geometry is not expected. Non-invasive surface-wave methods of $V_{s(30)}$ determination also provide an indication of uncertainties that may be associated with direct measurement of $V_s$. A study by Teague et al. [35] in Christchurch suggested that $\sigma_{\ln(V_{s(30)})}$ is typically less than approximately 0.05. A similar study by Vantassel et al. [36] in Wellington suggested slightly larger values but the calculated mean and standard deviations of representative site $V_{s(30)}$ were not based solely on lowest misfit profiles. Hence, an uncertainty factor of 5% is adopted for Method 1.

Two examples are provided in Appendix B to illustrate the application of Method 1 and the reader is referred to those for calculation details. Example 1 illustrates the calculation of $V_{s(30)}$ based on a $V_s$ profile determined from downhole $V_s$ measurements up to 25 m depth including required adjustments, such as the extension of the bottom measured $V_s$ to 30 m depth. Example 2 illustrates the calculation of $V_{s(30)}$ from MASW using 10 best-fit $V_s$ profiles. Note that the use of 10 best-fit $V_s$ profiles in this example is for demonstrating the application of this method and is not a general indication of the number of profiles needed to adequately account for the uncertainties in the $V_s$ profile and $V_{s(30)}$ at the site.

**Method 2: Evaluation of $V_{s(30)}$ based on Direct Field Measurement of $V_s$ to at least 15 m Depth**

In Method 2, the $V_s$ profile is established from direct $V_s$ measurement at the site from the ground surface to at least 15 m depth. Over the remaining depth of the profile to 30 m, $V_s$ can be estimated either using CPT or SPT data in conjunction with the empirical correlations for estimating $V_s$ recommended in the subsequent section on Method 3, the $V_{sz}$-$V_{s(30)}$ correlation recommended in this section under appropriate circumstances, or an authoritative geologic model for well-defined soil units in the area of interest. A good practice approach would expect to measure $V_s$ to 30 m depth or greater, and use Method 1. Method 2 is a compromise for cases when there are objective reasons to have measurements less than 25 m deep. In such cases, higher uncertainty factors (discussed subsequently) must be adopted which may result in higher design demands by enveloping design spectra across more site classes.

Estimates of $V_{s(30)}$ may be obtained using measured $V_s$ in conjunction with a correlation model between $V_{sz}$ and $V_{s(30)}$ (often referred to as a $V_{sz}$-$V_{s(30)}$ correlation), where $V_{sz}$ is the time-averaged $V_s$ to a depth $z$. The depth, $z$, of $V_{sz}$ corresponds to the maximum depth of $V_s$ measurement rounded down to the nearest whole number (e.g., 18.5 m is rounded down to 18 m) because model regression coefficients are often developed for whole number depths only. This approach utilises the empirical evidence that $V_{sz}$ and $V_{s(30)}$ are reasonably strongly correlated when $V_{sz}$ is defined for a depth $z \geq 15$ m. However, the procedure is statistical and therefore was developed to be accurate on average across many sites but would not be expected to result in a single correct $V_{s(30)}$ value on an individual site-specific basis. The use of $V_{sz}$-$V_{s(30)}$ correlations introduce additional uncertainties that must be accounted for when used in determining site class.

Comparison of two commonly used $V_{sz}$-$V_{s(30)}$ correlations, Boore [37] and Boore et al. [38], with direct $V_s$ measurement site investigation data in NZ was undertaken to determine an appropriate model for use in NZ, as well as quantify the uncertainty associated with using partial measurement of $V_s$ to estimate $V_{s(30)}$. Site investigation data was obtained from the NZ Geotechnical Database (NZGD) and other available sources. The $V_s$ profiles used have been obtained from sCPT, sDMT, downhole and crosshole measurements. This evaluation dataset required a minimum investigation depth of 29 m. For $V_s$ profiles that do not reach 30 m, the bottom layer $V_s$ was extended to 30 m (i.e., at most a 1 m extension). All profiles had the $V_s$ for z = 0-3 m depth adjusted to be equal to the average of the measured

$V_s$ between z = 2.5-3.5 m. The dataset consisted of 9 sCPT, 6 sDMT, 1 downhole and 1 crosshole investigations.

The applicability of the Boore [37] and Boore et al. [38] models were quantified by an investigation of residuals between predicted $V_{s(30)}$ as a function of $V_{sz}$ at depths between 10-29 m to measured $V_{s(30)}$. The residual as a function of depth, $z$, is defined as:

$$\Delta(z) = \ln\left(\frac{V^M_{s(30)}}{V^P_{s(30)}(z, V_{sz})}\right) \quad (1)$$

where, for a given $V_s$ profile, $\Delta(z)$ is the residual at depth $z$, $V^M_{s(30)}$ is the measured $V_{s(30)}$ (that may include extension of the bottom layer below 29 m), $V^P_{s(30)}(z, V_{sz})$ is the predicted $V_{s(30)}$ based on $V_{sz}$ at depth $z$, and ln is the natural logarithm such that all residuals are in natural logarithm units.

Figure 7a and 7b present the residuals for each $V_s$ profile, as a function of depth, for the Boore [37] and Boore et al. [38] models, respectively. The thick solid black line and grey-shaded areas indicate the model prediction bias and ±1 standard deviation (i.e., $\sigma_{\ln(V_{s(30)})}$) at each depth. The model prediction biases and standard deviations are compared for both models in Figures 7c and 7d, respectively. The published model standard deviations are also shown in Figure 7d as dashed lines and for each respective depth are larger than that from the NZ-specific residual analysis. An equivalent analysis was also performed considering $V_s$ profiles with a minimum investigation depth of 25 m, in order to include more data in the analysis, resulting in a total of 17 sCPT, 17 sDMT, 1 downhole and 3 crosshole investigations. The conclusions drawn from that analysis were the same as those based on the more stringent minimum investigation depth of 29 m, and hence these additional summary results are included in Figures 7c and 7d as the lighter coloured lines but the detailed analyses (equivalent to Figures 7a and 7b for the minimum investigation depth of 29 m) are not shown.

The Boore [37] model is recommended for estimating $V_{s(30)}$ based on $V_{sz}$, for $z \geq 15$ m as it is practically unbiased in prediction of $V_{s(30)}$ when the depth of investigation ranges between 15-29 m. No NZ-specific adjustments are required. In contrast, the Boore et al. [38] model tends to overpredict $V_{s(30)}$ and shows a rapid decrease in accuracy where the available depth of measured data is less. The Boore [37] model was derived from a California dataset of boreholes that reach at least 30 m depth and its linear functional form provides a more gradual increase in $V_s$ with depth that appears more consistent with prevalent NZ geotechnical conditions, at sites located within sedimentary basins, for which the correlation is expected to be used, compared to the parabolic functional form of Boore et al. [38] that provides a steeper increase in $V_s$ with depth. The Boore et al. [38] model was derived from a Japanese dataset (KiK-net) where stiffer sites (e.g., rock, rocklike, shallow soil over rock, stiff soils) are more prevalent and, based on current evidence, appears to be less consistent with NZ $V_s$ characteristics at sites located within sedimentary basins, for which the correlation is expected to be used. Consequently, the Boore [37] model should not be used if large impedance contrasts (e.g., soil to rock boundaries) and/or significant velocity reversals are expected within the extrapolated depth (i.e., between the depth of last $V_s$ measurement and 30 m).

The standard deviation associated with predicting $V_{s(30)}$ from $V_{s15}$ ranges between approximately 0.07-0.13 when considering both the values from the evaluation against NZ data (i.e., standard deviations of residuals when comparing predicted and observed values for NZ data) and the published values from the development of the Boore [37] and Boore et al. [38] models. Likewise, the standard deviation associated with predicting $V_{s(30)}$ from $V_{s25}$ ranges between approximately 0.03-0.04. The standard deviation expectedly decreases with increasing depth of investigation as more $V_s$ information is known over a larger depth range, such that $V_{s(30)}$ may be estimated with lower uncertainty. Between 15 m and 25 m, the variation in the standard deviation appears to be approximately linear. Therefore, a linear function appears suitable for the Method 2 uncertainty factor based on the depth of direct $V_s$ measurement obtained from ground investigation. Given the dataset used in the evaluation is not large and not representative of all site conditions in NZ, linear interpolation between a 15% uncertainty factor where $V_s$ is measured to a depth of 15 m and a 5% uncertainty factor where $V_s$ is measured to a depth of 25 m is adopted for Method 2.

For some in-situ tests commonly used to determine $V_s$ (e.g., sCPT), pre-drilling may be necessary to bypass stiff layers that could cause test refusal. This pre-drilling can occur either at the ground surface or at depth, depending on site conditions. However, it is essential that pre-drilling be used solely to bypass stiff layers and not as a method to circumvent other challenging

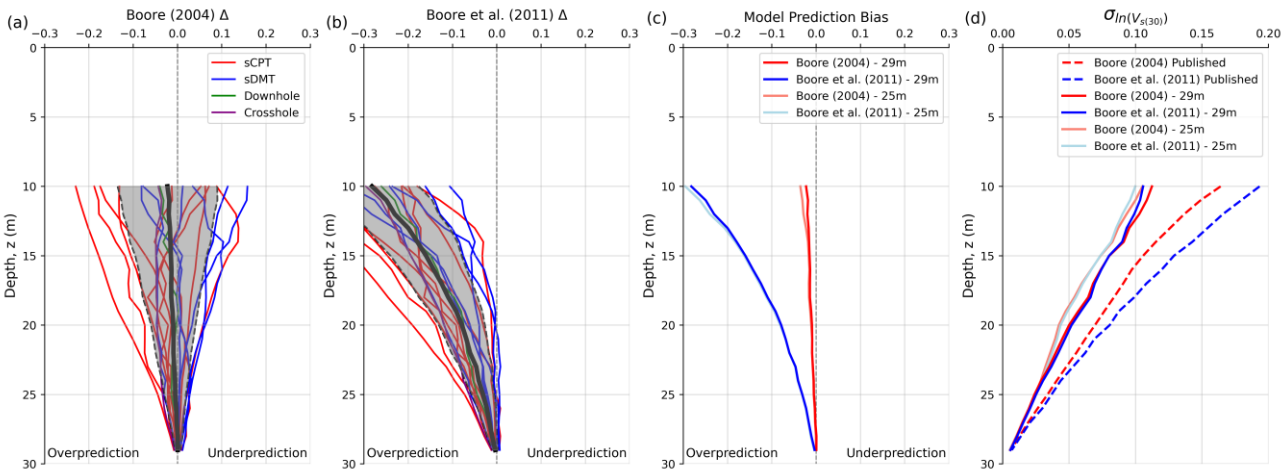


***Figure 7: Summary of $V_{sz}$-$V_{s(30)}$ model predictive capability: (a) predicted $V_{s(30)}$ residuals using Boore (2004) relative to measured $V_{s(30)}$ for 17 $V_s$ profiles; (b) predicted $V_{s(30)}$ residuals using Boore et al. (2011) relative to measured $V_{s(30)}$ for 17 $V_s$ profiles; (c) model prediction bias; and (d) standard deviation, $\sigma_{ln(V_{s(30)})}$. In panel (a) and (b), the thick solid black line indicates the model prediction bias and the shaded area represents ±1 standard deviation. In panel (d), the dashed lines indicate the published model standard deviations.***

or unfavourable site conditions, as this could introduce significant inaccuracies.

When pre-drilling without $V_s$ measurement has been appropriately employed, and the cumulative depth of pre-drilling does not exceed 5 metres, it is permissible to use the cumulative depth of $V_s$ measurements as a substitute for the depth of $V_s$ measurements from the ground surface for the determination of the uncertainty factor. For example, 5 m of pre-drill (without $V_s$ measurement) followed by 15 m of $V_s$ measurement would require an uncertainty factor of 15%. As another example, 5 m of $V_s$ measurement followed by 5 m of pre-drill without $V_s$ measurement and then a further 15 m of $V_s$ measurement would require an uncertainty factor of 10%. While this is not strictly consistent with the presented quantification of uncertainty, it is considered a practical alternative in the absence of a rigorous approach.

An authoritative geologic model, mentioned previously as a means to supplement the partially measured $V_s$ profile, refers to detailed geologic models that have been developed based on comprehensive studies and have been considered by local/regional authorities as an appropriate means for global site characterization in specific regions/areas. Such models should include a description of characteristic soil units, thickness of layers, and sufficient information to estimate an approximate range of $V_s$ based on available regional data for the geologic units of interest, for each soil layer over the depth of application of the geologic model. The use of such models is recommended only for cases in which well-established authoritative geologic models are considered to provide more reliable $V_s$ characterisation of the site as compared to the estimates based on empirical $V_{sz}$-$V_{s(30)}$ correlations. Such models will naturally have been comprehensively reviewed prior to their endorsement.

In areas with well-defined geologic units, the 15 m requirement can be relaxed to a shallower depth if established rock or gravelly formations are encountered and expected to continue over the remaining depth to 30 m. In such cases, $V_s$ = 500 m/s can be adopted for rock and $V_s$ = 350 m/s for stiff gravelly soils over the respective depth to 30 m for the calculation of $V_{s(30)}$. In such cases, the adopted uncertainty factor for $V_{s(30)}$ bounds should be that corresponding to measured $V_s$ over 15 m depth (i.e., 15%).

Two examples are provided in Appendix B to illustrate the application of Method 2 in practice. Example 3 illustrates the calculation of $V_{s(30)}$ based on a $V_s$ profile determined from downhole $V_s$ measurements to a depth of 18.5 m and a simple application of the Boore [37] $V_{sz}$-$V_{s(30)}$ correlation to obtain $V_{s(30)}$. Example 4 illustrates the calculation of $V_{s(30)}$ from a $V_s$ profile determined from downhole measurements up to 21 m depth supplemented with CPT-inferred $V_s$ at greater depths. In this specific example, the bottom of the soil layer within which the $V_s$ measurements terminate can be identified in the CPT trace and therefore the $V_s$ for the last measured layer is extended to the bottom of that soil layer under the assumption that it is likely to be more accurate than CPT-inferred $V_s$. Below the bottom of this soil layer, the CPT-inferred $V_s$ is adopted.

**Method 3: Evaluation of $V_{s(30)}$ Primarily based on Inferred or Estimated $V_s$**

In Method 3, the $V_s$ profile is inferred from CPT or SPT measurements, or a combination of such penetration measurements and measured $V_s$, provided CPT, SPT or $V_s$ data are available to a depth of at least 20 m, but the depth of measured $V_s$ is insufficient for Method 1 or Method 2.

Similar to Method 2, in areas with well-defined geologic units, the 20 m requirement can be relaxed to a shallower depth if established rock or gravelly formations are encountered and expected to continue over the remaining depth to 30 m. In such cases, $V_s$ = 500 m/s can be adopted for rock and $V_s$ = 350 m/s for stiff gravelly soils over the respective depth to 30 m for the calculation of $V_{s(30)}$.

*CPT-based Correlations*

When using Method 3, it is important to carefully interpret penetration test data. For example, shallow refusal of a CPT sounding does not necessarily prove the absence of softer layers at greater depth. In cases of CPT refusal, it may be necessary to either pre-drill shallow dense layers or switch to machine boreholes and SPT sampling, and demonstrate that softer layers are not encountered at greater depth. If pre-drilling is followed by CPT sounding, then properties of the soils drilled through should be assessed utilising SPT. In cases when high-resistance layers are encountered in the deposit, for which CPT and SPT are not viable options, $V_s$ estimates can be obtained either from authoritative geologic models or using data from adjacent sites, provided that equivalent soil units are confirmed at both sites, and the thickness of the subject layers are well defined. If geologic models or data from adjacent sites are not available, and CPT/SPT refusal is encountered over depth intervals with cumulative depth of less than 5 m, a default value of $V_s$ = 250 m/s is recommended to be adopted over the depth of refusal. Provided the cumulative depth of pre-drilling is less than 5 m, then the relevant parts of the pre-drilled depths can be considered to be a part of the 20 m of investigation required for use of Method 3.

To determine the applicability of CPT-$V_s$ correlations in NZ, several models were scrutinized against site investigation data obtained from the NZGD and other available sources. This evaluation dataset required co-located or closely located CPT and $V_s$ measurements to allow comparison between $V_{s(30)}$ based on measured and predicted $V_s$. An additional criterion required at least 14 m of both CPT and $V_s$ measurements, using the Boore [37] $V_{sz}$-$V_{s(30)}$ correlation to convert the $V_{sz}$ at the maximum depth of investigation to a $V_{s(30)}$ as needed. 83 sCPT met the criteria above and 46 sites had separate CPT and $V_s$ measurements from sDMT that were considered to be located sufficiently close for inclusion in the evaluation dataset (35 less than 10 m and 11 between 11-46 m, approximately). Potential differences in the soil profiles sampled by CPT and sDMT tests due to spatial offsets are acknowledged. To mitigate the impact of these differences, we assessed the similarity in $V_s$ layering relative to changes in the CPT trace and evaluated whether variations in $V_s$ and CPT measurements ($q_c$ and $f_s$) were consistent when compared to the variability observed in sCPT data (where CPT and $V_s$ measurements are co-located). Other CPT-sDMT pairs with separation distances exceeding 10m, and where geology or stratigraphy appeared sufficiently different, were excluded from the dataset used in this analysis. Figure 8 shows the locations where the data was obtained, primarily from Canterbury, Tauranga, Waikato and Auckland. Figure 9 shows the distribution of CPT and $V_s$ maximum investigation depths.

Figure 10 presents plots of predicted $V_{s(30)}$ using CPT-$V_s$ correlations against $V_{s(30)}$ based on measured $V_s$, both with "extrapolation" via the Boore [37] $V_{sz}$-$V_{s(30)}$ correlation where required, for the recommended CPT-$V_s$ correlation models. The solid grey line indicates equality between prediction and measurement, while the dashed grey lines indicate 30% uncertainty bounds. For sites in Christchurch, the McGann et al. [39] (M15) model, in Figure 10a, is recommended for shallow non-gravelly soils since the comparison indicated that it performed best against that regional subset of data. M15 may also be appropriate to use in other regions of NZ where similar soil characteristics (young, Holocene-aged alluvial deposits of fluvial origin) and ground conditions like those prevalent in Christchurch exist. Banks Peninsula loess found in

Christchurch was identified to be systematically different from sedimentary soils in Christchurch, and hence the McGann et al. [40] (M18) model that was developed specifically for applications to such soils is recommended, as shown in Figure 10b.

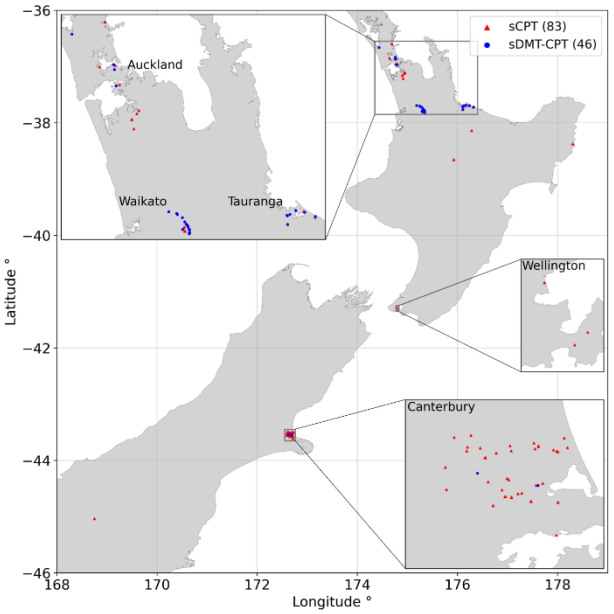


***Figure 8: Location of site investigation data used for evaluation of CPT-$V_s$ correlations.***

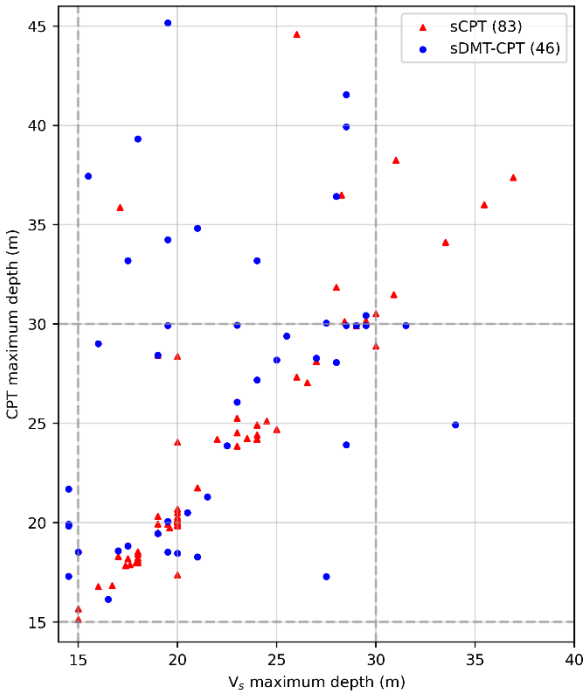


***Figure 9: Maximum depth of $V_s$ measurement versus maximum depth of CPT data used for evaluation of CPT-$V_s$ correlations.***

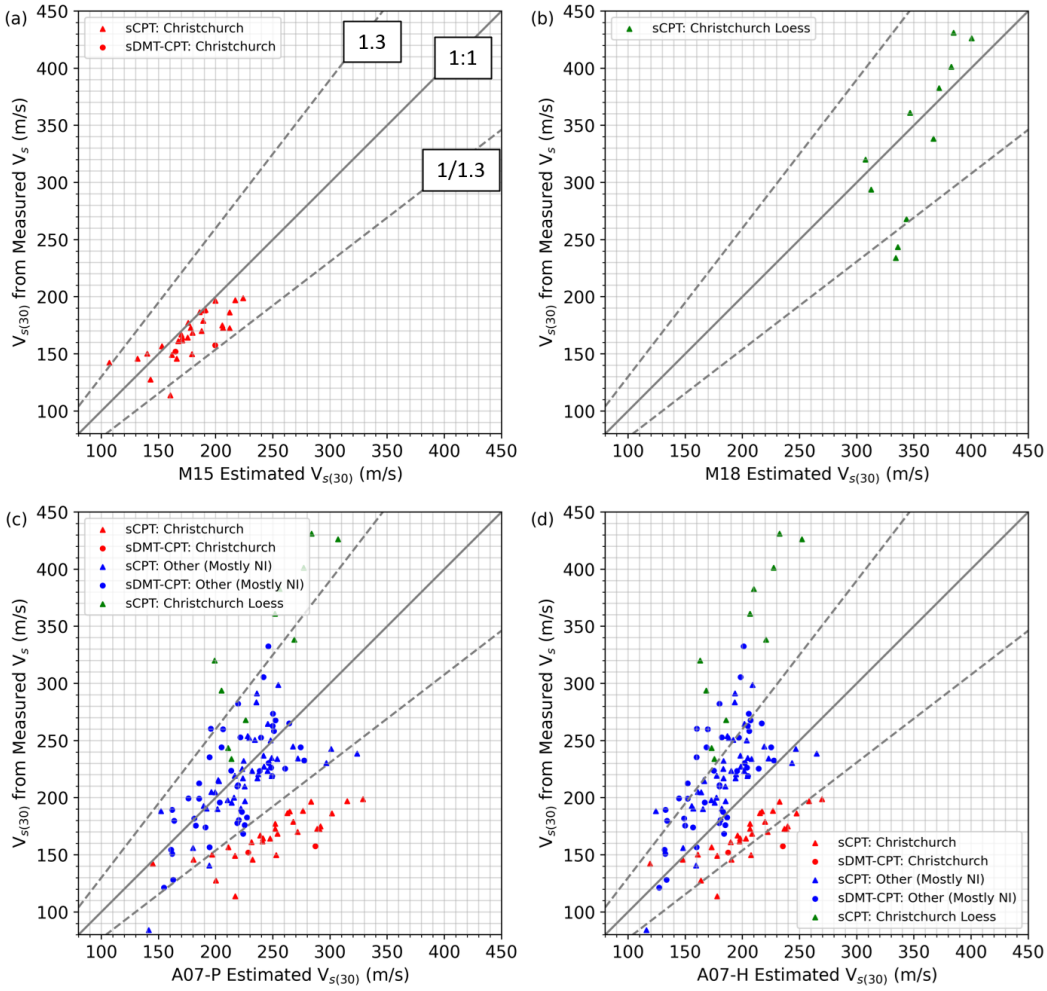


***Figure 10: Comparison of predicted $V_{s(30)}$ against $V_{s(30)}$ from measured $V_s$ from the evaluation dataset for: (a) McGann et al. (2015) model, (b) McGann et al. (2018) model, (c) Andrus et al. (2007) Pleistocene model, and (d) Andrus et al. (2007) Holocene model.***

The Andrus et al. [41] model, derived from a combination of Holocene and Pleistocene data, is recommended for application to other regions of NZ, except for those similar to Christchurch alluvial soils as discussed above. The Andrus et al. [41] Pleistocene (A07-P) model was found to match the available data outside of Christchurch best, as shown in Figure 10c, and is recommended for sites comprising more than 15 m of Pleistocene soils from the ground surface to 30 m depth. The Andrus et al. [41] Holocene (A07-H) model (developed from regression against Pleistocene and Holocene data but with the Holocene scaling factor) is recommended for sites with younger Holocene deposits exceeding a depth of at least 15 m. This is shown in Figure 10d.

Several other models were evaluated against the dataset but are not recommended for use in NZ. The Hegazy and Mayne [42] CPT-$V_s$ correlation model was found to be sensitive to particular combinations of CPT parameters, likely due to its functional form. Therefore, it is not recommended currently, since stability in $V_s$ estimates is preferred for the expected applications. The Robertson [43] CPT-$V_s$ correlation model showed systematic biases when compared to several NZ regional datasets and therefore is not currently recommended either.

Both CPT and $V_s$ measurements have larger inaccuracies at shallow depths, especially at depths shallower than approximately 3 m below the ground surface. Reasons for this include low overburden stress, experimental errors and challenges in the interpretation of measured data (Andrus et al. [41], McGann et al. [39]). Therefore, when using a CPT-$V_s$ correlation to determine $V_{s(30)}$, it is recommended for the value of $V_s$ between 0-3 m to adopt the average of the estimated $V_s$ between 2.5-3.5 m. This recommendation is aimed to prevent skewing of $V_{s(30)}$ as a result of the potential erratic nature of CPT measurements or absence of CPT measurements at shallow depths, as well as biases associated with methodological assumptions.

*SPT-based Correlations*

There is currently no robust NZ-specific SPT-$V_s$ correlation that is suitable for nationwide application, and no international models have been rigorously validated against NZ data. In the absence of a validated model against NZ data, the Kwak et al. [44] SPT-$V_s$ correlation model, derived using a substantial dataset from Japan, is recommended for clay, silt, sand, and gravel soils, until robust and comprehensive NZ-specific models are developed. The regression coefficients of Kwak et al. [44] are soil-type dependent, and also dependent on raw SPT blowcount ($N$) with a set of coefficients for $1 \leq N < 50$ and a set of coefficients for $N \geq 50$. However, it is recommended to only use the coefficients for $1 \leq N < 50$ because the coefficients for $N \geq 50$ are poorly constrained. For SPT measurements of $N \geq 50$, the coefficients for $1 \leq N < 50$ should be used assuming $N = 50$.

For gravelly soils, the energy-corrected formulation of the Ohta and Goto [45] model, as presented in Wair et al. [46], can be used as an alternative to Kwak et al. [44] if the soil age is known since it has separate model coefficients for Holocene and Pleistocene gravels. Despite using a more limited dataset, mostly from alluvial plains in Japan, the Ohta and Goto [45] model is, on average, broadly consistent with the Kwak et al. [44] model for gravelly soils. The Ohta and Goto [45] Holocene model yields lower $V_s$ than the Ohta and Goto [45] Pleistocene model, and the Kwak et al. [44] model, that was developed using both Holocene and Pleistocene data, typically predicts intermediate values.

*Uncertainty in $V_{s(30)}$ Estimates*

Significant scatter in $V_{s(30)}$ estimates is expected when using correlations between $V_s$ and geotechnical penetration resistance (both CPT and SPT). This arises from many factors including the discrepancy between a measured proxy for a large-strain strength parameter over limited depth interval (i.e., penetration resistance) and predicted low-strain stiffness parameter (i.e., $V_s$) over large volume of soils, limited data used in the development of models, the relatively simple model functional forms, and inherent soil variability, among others. Differences in regression coefficients and parameter scaling between models are also expected given that density and depth (i.e., overburden stress) effects are not independent. Hence, Method 1 and Method 2 that use direct measurement of $V_s$ are preferred over the use of correlation-based Method 3 estimates.

The uncertainty required to be considered with Method 3 reflects the absence of directly measured $V_s$ at the site, the use of $V_s$ correlations with penetration resistance measurements, and extrapolation of a partially inferred profile that does not extend to 30 m depth. Limited studies have quantified the accuracy of $V_{s(30)}$ estimates based on SPT-$V_s$ and CPT-$V_s$ correlations. Citing the FEMA NEHRP provisions [47], recent studies of SPT-$V_s$ correlations for California [48] and Japan [44] have compared $V_{s(30)}$ obtained from measured $V_s$ profiles with correlation-based estimates of $V_{s(30)}$ using their respective datasets. These comparisons found standard deviations, $\sigma_{\ln V_{s(30)}}$, of 0.221 and 0.26 for Brandenberg et al. [48] and Kwak et al. [44], respectively. Considering lognormal percentiles corresponding to $\pm 1\sigma_{\ln(V_{s(30)})}$, this suggests there to be approximately 68% chance that the actual value of $V_{s(30)}$ is between $V_{s(30)}/1.3$ and $1.3V_{s(30)}$ [8,47]. The adopted 30% uncertainty factor associated with Method 3 is partially based on this rationale with further evidence from the CPT-$V_s$ correlation analysis presented in Figure 10 where most of the $V_{s(30)}$ calculated from measured $V_s$ were within 30% of predicted $V_{s(30)}$ from the relevant recommended models. For use of Method 3, it is critically important that the geotechnical site investigation (e.g., CPT and SPT) rigorously follows required standards of practice (e.g., in measurement, data acquisition and interpretation, modelling and so forth; NZGS/MBIE Module 2 [27]) otherwise resulting $V_s$ estimates would not be of satisfactory quality.

*Application of the Proposed Correlations*

Since $V_{s(30)}$ is a site characterisation parameter that reflects the overall stiffness characteristics of deposits from the ground surface to 30 m depth, it is quite different from CPT or SPT sounding data that provide local measures of soil resistance at a particular depth in the profile. In this context, $V_{s(30)}$ typically shows much smaller spatial variability across a given site as compared to CPT or SPT profiles. For this reason, for generally uniform sites from a global geology perspective (substantially different site classes are unlikely across the site), when multiple CPT or SPT profiles are used to infer the representative $V_{s(30)}$ of the site via Method 3, it is appropriate to determine a $V_s$ profile separately for each CPT or SPT profile, calculate $V_{s(30)}$ for each profile, and then calculate the weighted-average of the $V_{s(30)}$ across all profiles. The $V_{s(30)}$ of each profile should be weighted by the maximum depth of investigation as a proxy for the relative level of information used and accuracy in the estimate of each $V_{s(30)}$. There is no need to account for the spatial variability of CPT/SPT data across the site, as such effects are already accounted for through the 30% uncertainty factor adopted when estimating $V_{s(30)}$ via Method 3.

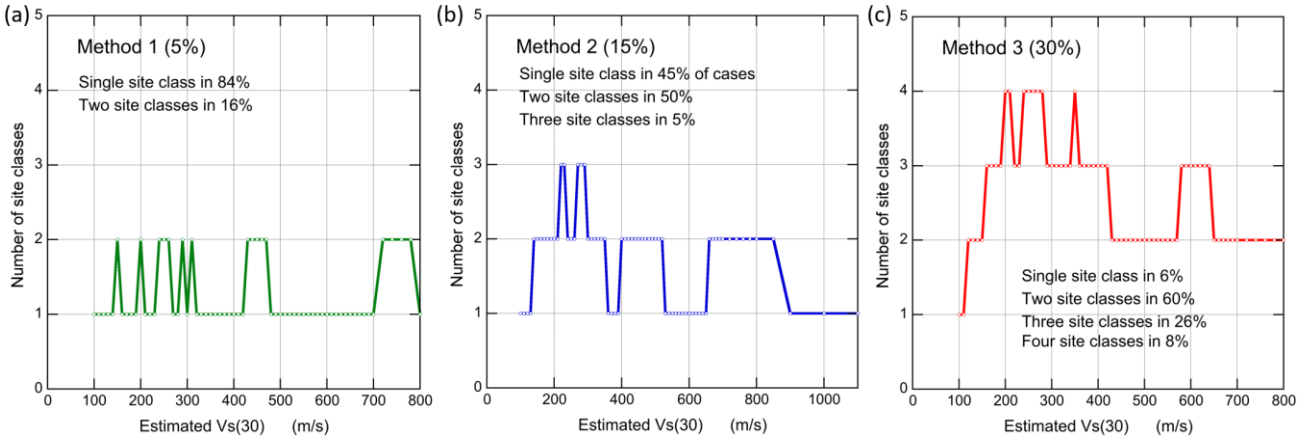


***Figure 11: Number of site classes resulting from the adopted classification scheme for different 'central values' of $V_{s(30)}$ and evaluation methods for $V_s$: (a) Method 1; (b) Method 2; and (c) Method 3.***

Four examples are provided in Appendix B to illustrate the application of Method 3 and the reader is referred to those for calculation details. Example 5 illustrates the calculation of a representative $V_{s(30)}$ for a site where three CPTs are conducted and have different termination depths, at 20 m, 24 m and 25 m. In this example, the $V_{s(30)}$ is calculated for each profile, including extension of the $V_s$ measured in the last layer to 30 m, and a weighted average value based on the maximum depth of each CPT is used to calculate the representative $V_{s(30)}$ for the site. Example 6 illustrates the calculation of a representative $V_{s(30)}$ for a site with two CPTs that experience refusal in a shallow stiff layer at 12 m depth. The stiff shallow layer is bypassed with pre-drilling to 16 m depth and is assigned a default $V_s$ = 250 m/s, which is an available option in the absence of data over a cumulative refusal depth of less than 5 m. CPT soundings are continued below this soil layer to a termination depth of 20 m. Example 7 illustrates the calculation of a representative $V_{s(30)}$ for a site with two CPTs that terminate at 20 m on a deep stiff layer in conjunction with an authoritative geologic model that suggests a range of $V_s$ that should be considered for each relevant soil layer. Lastly, Example 8 illustrates the calculation of $V_{s(30)}$ using SPT-$V_s$ correlations. Since SPT have coarser (discrete) sampling over depth than CPT, particular attention must be paid to the boundaries between soil layers when using SPT-$V_s$ correlations, so that a measurement in one soil layer is not used to estimate $V_s$ in a different soil layer. Few measurements would be obtained at shallow depths (i.e., often only one at depths less than 3 m below ground surface), hence it is important to scrutinise the quality of the sampling and the suitability of the inferred $V_s$ value based on the soil types encountered in the boreholes.

### Multiple Site Class

Where the uncertainty in $V_s$ estimates results in a range of $V_{s(30)}$ values that encompass two or more site classes, then multiple site classes should be adopted for the site. The design spectrum for such cases should be determined as the envelope of the design spectra of the relevant multiple site classes based on the estimated range of $V_{s(30)}$ values (i.e., the maximum spectral acceleration at each period across the design spectra of all encompassed site classes). In principle, the approach used to envelope spectra for Multiple Site Classes is similar to that shown for the Default Site Class in Figure 6.

Figure 11 comparatively illustrates the number of site classes obtained when using Method 1, Method 2 and Method 3, for establishing the $V_s$ profile at the site as a function of the 'central value' of $V_{s(30)}$ (x-axis). When the $V_s$ profile is established based on direct $V_s$ measurements over the 'full' profile (Method 1), the uncertainty in $V_{s(30)}$ is the lowest (5%), and consequently the estimated range of $V_{s(30)}$ is relatively small. Thus, when Method 1 is employed, in 84% of the depicted cases in Figure 11a a single site class is obtained; for the remaining 16% of the cases, the estimated range of $V_{s(30)}$ values spans two site classes. As illustrated in Figure 11a, two site classes are identified when the estimated 'central value' of $V_{s(30)}$ is in the vicinity of the $V_{s(30)}$ thresholds separating different site classes (i.e., in the vicinity of $V_{s(30)}$ = 150, 200, 250, 300, 450 and 750 m/s).

Conversely, for Method 3 (Figure 11c) in which the $V_s$ profile is inferred from CPT or SPT data, and consequently the uncertainty in $V_{s(30)}$ is the largest (30%), in 94% of the cases multiple site classes are obtained. In one third of the cases, the estimated range of $V_{s(30)}$ values would span over three or four site classes. Importantly, the large number of site classes (i.e., three or four) are obtained for $V_{s(30)}$ values in the range between 160 m/s and 420 m/s, which includes the most commonly encountered conditions for populated regions across New Zealand (e.g., Kaiser et al. [21], Wotherspoon et al. [22]; NZ Geotechnical Database; and insights from Foster et al. [23] and Perrin et al. [24])). Thus, Method 3 will often result in a design spectrum that is defined by the envelope of the design spectra for at least three of Site Classes III, IV, V and VI.

For Method 2, Figure 11b shows the number of site classes that must be considered when the uncertainty in $V_{s(30)}$ is 15%. Note that 15% is the maximum uncertainty for Method 2, in cases when $V_s$ is measured only up to a depth of 15 m. In this case, 95% of the cases will result in one or two site classes, and only 5% of cases will result in three site classes.

To improve the accuracy in the site characterisation and allow for a selection of more narrowly defined design spectra, it is recommended to employ direct $V_s$ measurements at the site (that is Method 1 and Method 2). This approach will substantially reduce the uncertainty in $V_{s(30)}$ estimates and may eliminate the need for adopting potentially conservative design spectra across multiple site classes.

## DISCUSSION

### Site Effects in Design Spectra

*Site effects* is a general term that includes various factors that may materially impact the severity of ground motion and response spectra characteristics (e.g., characteristics of shallow soils, sedimentary basin effects, basin-edge effects, topographic effects). Variations in ground motions and the influence of such

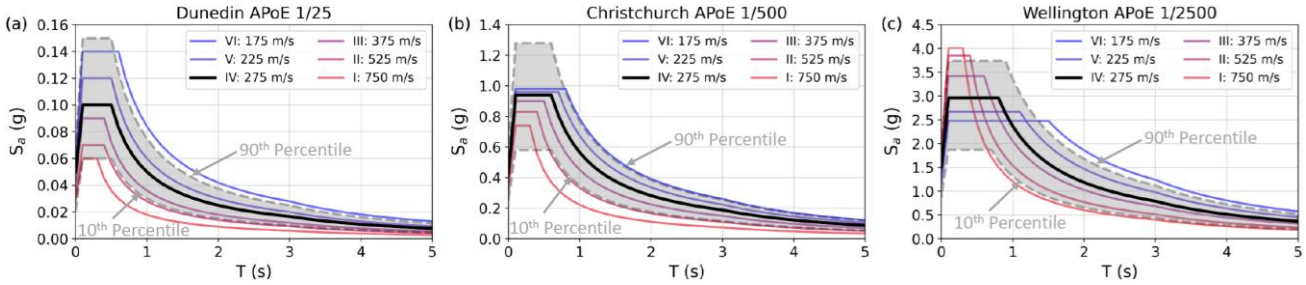


***Figure 12: Uncertainty in uniform hazard spectra within the design spectra framework, illustrated with 10th and 90th percentile fitted spectra for Site Class IV ($V_{s(30)}$ = 275 m/s) compared to the range of code spectra across site classes. Three combinations of locations and annual probability of exceedances are shown: (a) Dunedin APoE 1/25; (b) Christchurch APoE 1/500; and (c) Wellington APoE 1/2500.***

effects in response spectra are implicitly accounted for through the GMMs used in PSHA, as they are developed based on ground motion records that contain such effects. However, it is important to recognize that in the response spectra derived from PSHA (including uniform hazard spectra and design spectra) such effects are averaged across a large number of records, which include basin effects of various intensities, basin geometries and subsurface stratigraphy. In this context, the design spectra derived from NSHM2022 represent basin effects in a globally-averaged sense, which is consistent with the overall philosophy of using the mean results from NSHM2022 adopted in the TS 1170.5. For high importance structures, site-specific studies considering detailed basin characteristics and subsurface stratigraphy provide an alternative approach that reduces uncertainties by quantifying the full range of such effects for the specific characteristics at the site of interest.

**Proposed Site Classes in the Context of Uncertainty in PSHA**

A comparative examination between the effects of site classes on design spectra and the uncertainty in the uniform hazard spectra themselves provides context on the significance of $V_{s(30)}$ uncertainty required in site class determination, including the use of a multiple site class definition. For this purpose, Figure 12 presents the design spectra for Site Classes I to VI, for Dunedin APoE 1/25, Christchurch APoE 1/500 and Wellington APoE 1/2500, which effectively represent low, moderate and high shaking intensities, respectively. The design spectra for Site Class IV ($V_{s(30)}$ = 275 m/s), shown with bold lines, are used as a baseline for comparison. The lower bound and upper bound lines of the shaded area indicate 10th and 90th percentile design spectra (i.e., derived from 10th and 90th percentile uniform hazard spectra) for Site Class IV, which together with the mean spectra (bold line) are indicative of the variation of uniform hazard spectra obtained from NSHM2022 for $V_{s(30)}$ = 275 m/s (i.e., Site Class IV). It is apparent that the variation in response spectra obtained in NSHM2022 for a single $V_{s(30)}$ (i.e., site class) is greater than the variation in design spectra between different site classes. These comparisons imply that even when adopting multiple site classes for a given site due to the uncertainties in site classification, the adopted envelope spectrum would not be overly conservative, as it will be most likely in the interquartile range (i.e., middle 50%) of spectral values for the most relevant site class.

**Comparisons Between TS 1170.5 and NZS 1170.5**

NZS 1170.5 is based on the 2002 NZ NSHM [49], and adopted a single empirical GMM (McVerry et al. [50]) with an alphabet-based Site Class definition that was eventually adopted in NZS 1170.5. $V_{s(30)}$ was not a comprehensively considered site parameter in site class determination and not all site classes had $V_{s(30)}$ criteria. Instead, other geotechnical engineering factors such as unconfined compressive strength, undrained shear strength, depth of soil, natural site period, and geotechnical penetration measurements are used. Hence, a rigorous comparison between TS 1170.5 design spectra (derived from NSHM2022 uniform hazard spectra) and NZS 1170.5 design spectra is not possible, as there is no direct correlation between NZS 1170.5 site classes and $V_{s(30)}$, which essentially makes the NZS 1170.5 site classification scheme incompatible with the PSHA methodology underpinning NSHM2022. Kaiser et al. [21] illustrates this absence of direct correlation by presenting the distribution of $V_{s(30)}$ values for NZS 1170.5 Site Class C (Figure 6a in Kaiser et al. [21]) and Site Class D (Figure 6b in Kaiser et al. [21]) for sites in central Wellington. For NZS 1170.5 Site Class C, $V_{s(30)}$ takes a wide range of values from 200 m/s to 1000 m/s, and is predominantly between 250 m/s and 450 m/s. NZS 1170.5 Site Class D has $V_{s(30)}$ values mostly from 200 m/s to 400 m/s, which stretches across Site Classes III, IV and V of TS 1170.5. To allow for some meaningful comparisons between the TS 1170.5 and NZS 1170.5 design spectra, the most compatible site classes between TS 1170.5 and NZS 1170.5 were used (i.e., VI and E, V and D, III and C, II and B, and I and A). The most compatible site classes were based on means, medians and ranges of $V_{s(30)}$ for each NZS 1170.5 site class across other studies (e.g., Kaiser et al. [21] and Wotherspoon et al. [22]).

The difference at the individual site class level is illustrated in Figure 13 that presents spectral acceleration ratios between the most compatible site classes between TS 1170.5 and NZS 1170.5. The results are summarised as the mean ratio across 12 locations in NZ corresponding to significant population centres (the same locations as for Figure 5), for APoE 1/25, 1/500 and 1/2500. The ±1 standard deviation of the spectral ratios between Site Classes II/B and VI/E (shown by the shaded areas) are included because they are typically the largest and smallest, respectively, across the period range considered, and for each APoE. The differences here between TS 1170.5 and NZS 1170.5 design spectra are primarily due to both seismic source and ground motion models (as well as method of design spectra development from uniform hazard spectra), but the goal is to show how the design hazard has changed between NZS1170.5 and TS 1170.5 for any particular site using the most compatible site classes as the association.

In general, at short periods the ratios can be relatively large and exhibit some significant fluctuations due to differences in constant acceleration plateau values and corner periods. At longer periods, the ratios become more uniform across periods. At APoE 1/25, the TS 1170.5 design spectral accelerations are typically similar to or smaller than NZS 1170.5 with the exception of spectral acceleration ratios at short periods for a few site classes. At APoE 1/500, all site classes have an average ratio greater than or equal to 1. Soft rock (II/B) and stiff soil (III/C) having the largest ratios, mostly ranging from approximately 1.7 to 2.1. Very soft soils (VI/E) have relatively small ratios, closer to 1. Lastly, at APoE 1/2500, similar trends

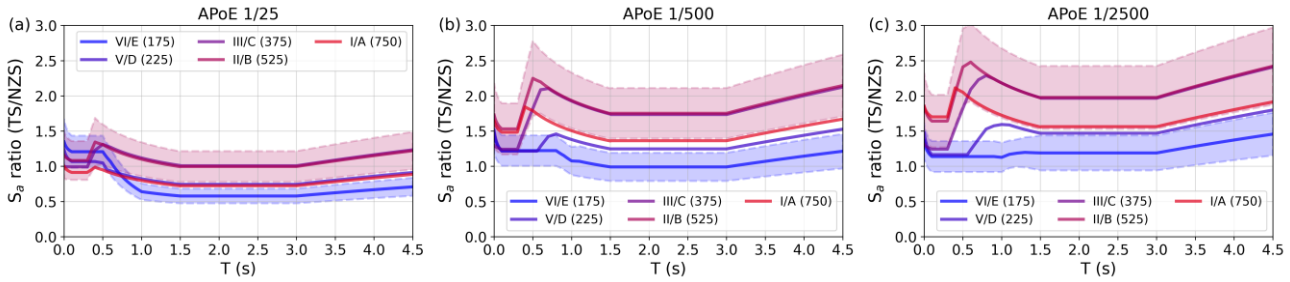


***Figure 13. Spectral ratios between the most compatible TS 1170.5 and NZS 1170.5 site classes across 12 test locations for: (a) APoE 1/25; (b) APoE 1/500; and (c) APoE 1/2500.***

to APoE 1/500 are present. As APoE decreases (from 1/25 to 1/500 to 1/2500), the standard deviation across the 12 locations tends to increase for all site classes.

### Limitations of Scope and Further Details

This paper aims to provide an overview of the proposed site class methodology for the TS 1170.5 design spectra and to facilitate its implementation into practice. Given this limited scope and specific objectives, many important details and situations discussed in the TS 1170.5 have been omitted. The reader is referred to Sections 3.1.3 and C3.1.3 of TS 1170.5 and its accompanying commentary for further details including scenarios and situations that have not been covered in this paper.

## CONCLUDING REMARKS

Site effects strongly influence ground motions and require appropriate consideration in code provisions for seismic design actions. The NSHM2022 represented a fundamental shift in the incorporation of site effects relative to the PSHA underpinning the preceding NZS 1170.5. Therefore, an updated methodology has been advised in the TS 1170.5 that incorporates NSHM2022 into an update of the NZ Building Code B1/VM1. The only explicitly-defined site parameter used in NSHM2022 is $V_{s(30)}$, and therefore, it is the principal site parameter that TS 1170.5 site classes are based upon. The site classes adopted in TS 1170.5 provide gradual and smooth transitions across design spectra for different site classes, for low, moderate and high shaking intensities. Importantly, the site classification methodology allows for a robust incorporation of site effects, yet in a practical manner appropriate for engineering design practice.

Several methods for obtaining a $V_s$ profile, measured or inferred, and subsequent calculation of $V_{s(30)}$ were recommended with justification tied to comprehensive scrutiny of candidate models and their comparative evaluation against NZ data, research literature, and international code provisions. Each method is associated with a different uncertainty factor that must be considered in site class determination to reflect the uncertainties. This results in a range of $V_{s(30)}$ values that must be considered and could span several site classes, resulting in a multiple site class definition with an envelope design spectrum. In the context of the uncertainty associated with site classes, a comparison is made to equivalent design spectra based on 10$^{th}$ and 90$^{th}$ percentile uniform hazard spectra which illustrates that the uncertainty within the uniform hazard spectra themselves is approximately on the same order as the uncertainty implied by multiple site classes, and therefore the latter is not necessarily overly conservative. For sites with ground conditions not well-represented within the PSHA performed for NSHM2022 or reduced uncertainty is desired due to the structure being considered as critical or high priority, site-specific seismic hazard studies are recommended.

While this article provides an outline and discussion on the recommended methodology for site classification, the reader is referred to TS 1770.5 and accompanying commentary for details on the site classification methodology and its application.

## ACKNOWLEDGMENTS

The authors would like to thank all members of the Seismic Risk Working Group for their input throughout the development of TS 1170.5. The authors would like to give specific thanks to Anne Hulsey and Tom Francis for providing NSHM results and derived products. The authors would also like to thank Christopher de la Torre, Riwaj Dhakal, Christopher McGann, Andrew Stolte, Nick Traylen, Frederick Wentz and Liam Wotherspoon for help with obtaining and interpreting geotechnical data, and understanding geotechnical models. The New Zealand Geotechnical Database, from which most of the data used in this article was obtained, has been an extremely valuable repository of data and the authors would like to thank the developers, maintainers, and contributors to the database. Lastly, the authors are thankful to Liam Wotherspoon, Jon Stewart and Nick Traylen for providing comments towards the improvement of this manuscript through their review.

## REFERENCES

1 Gerstenberger MC, Bora S, Bradley BA, DiCaprio C, Kaiser A, Manea EF, Nicol A, Rollins C, Stirling MW, Thingbaijam KKS, Van Dissen RJ, Abbott ER, Atkinson GM, Chamberlain C, Christophersen A, Clark K, Coffey GL, de la Torre CA, Ellis SM, Fraser J, Graham K, Griffin J, Hamling IJ, Hill MP, Howell A, Hulsey A, Hutchinson J, Iturrieta P, Johnson KM, Jurgens VO, Kirkman R, Langridge RM, Lee RL, Litchfield NJ, Maurer J, Milner KR, Rastin S, Rattenbury MS, Rhoades DA, Ristau J, Schorlemmer D, Seebeck H, Shaw BE, Stafford PJ, Stolte AC, Townend J, Villamor P, Wallace LM, Weatherill G, Williams CA and Wotherspoon LM. (2024). "The 2022 Aotearoa New Zealand National Seismic Hazard Model: Process, overview and results". *Bulletin of the Seismological Society of America*, **114**(1): 7-36. https://doi.org/10.1785/0120230182

2 Standards New Zealand (2004). "*NZS 1170.5: Structural Design Actions. Part 5: Earthquake Actions - New Zealand*". Standards New Zealand, Wellington, NZ, 76pp. https://www.standards.govt.nz/sponsored-standards/building-standards/NZS1170-5

3 Housner GW (1941). "Calculating the response of an oscillator to arbitrary ground motion". *Bulletin of the Seismological Society of America*, **31**(2): 143-149. https://doi.org/10.1785/BSSA0310020143

4 Biot MA (1942). "Analytical and experimental methods in engineering seismology". *In Proceedings of the American Society of Civil Engineers*, **68**(1): 49-69.

5 Housner GW (1959). "Behavior of structures during earthquakes". *Journal of the Engineering Mechanics Division*, **85**(4): 109-129. https://doi.org/10.1061/JMCEA3.0000102

6 Hayashi S, Tsuchida H and Kurata E (1972). *Average response spectra for various subsoil conditions*. Mcgraw Hill Book Company.

7 Seed HB, Ugas C and Lysmer J (1976). "Site-dependent spectra for earthquake-resistant design". *Bulletin of the Seismological Society of America*, **66**(1): 221-243. https://doi.org/10.1785/BSSA0660010221

8 ASCE (2022). "Minimum Design Loads and Associated Criteria for Buildings and Other Structures, ASCE/SEI 7-22". ASCE, Reston, VA. https://doi.org/10.1061/9780784415788

9 Baker J, Bradley B and Stafford P (2021). *Seismic Hazard and Risk Analysis*. ISBN 978-1-108-42505-6, Cambridge University Press, United Kingdom, 600pp. https://doi.org/10.1017/9781108425056

10 Bozorgnia Y, Abrahamson NA, Al Atik L, Ancheta TD, Atkinson GM, Baker JW, Baltay A, Boore DM, Campbell KW, Chiou BS, Darragh R, Day S, Donahue J, Graves RW, Gregor N, Hanks T, Idriss IM, Kamai R, Kishida T, Kottke A, Mahin SA, Rezaeian S, Rowshandel B, Seyhan E, Shahi Shrey, Shantz, Silva W, Spudich P, Stewart JP, Watson-Lamprey J, Wooddell K and Youngs R (2014). "NGA-West2 Research Project". *Earthquake Spectra*, **30**(3): 973-987. https://doi.org/10.1193/072113EQS209M

11 Bozorgnia Y, Abrahamson NA, Ahdi SK, Ancheta TD, Al Atik L, Archuleta RJ, Atkinson GM, Boore DM, Campbell KW, Chiou BS, Contreras V, Darragh RB, Derakhshan S, Donahue JL, Gregor N, Gulerce Z, Idriss IM, Ji C, Kishida T, Kottke AR, Kuehn N, Kwak D, Kwok AO, Lin P, Macedo J, Mazzoni S, Midorikawa S, Muin S, Parker GA, Rezaeian S, Si H, Silva WJ, Stewart JP, Walling M, Wooddell K and Youngs RR (2022). "NGA-Subduction research program". *Earthquake Spectra*, **38**(2): 783-798. https://doi.org/10.1177/87552930211056081

12 BSSC (Building Seismic Safety Council) (2003) "NEHRP Recommended Provisions for Seismic Regulations for New Buildings and Other Structures (FEMA 450)", Washington DC.

13 BS EN 1998-1:2004 (2004) "Eurocode 8. Design of structures for earthquake resistance". European Committee for Standardization (CEN), Brussels.

14 NBCC (2015). "National Building Code of Canada". National Research Council of Canada, Ottawa. https://doi.org/10.4224/40002005

15 ASCE (2016). "Minimum Design Loads and Associated Criteria for Buildings and Other Structures, ASCE/SEI 7-16". ASCE, Reston, VA. https://doi.org/10.1061/9780784414248

16 Stirling MW, McVerry GH and Berryman KR (2002). "A New Seismic Hazard Model for New Zealand". *Bulletin of the Seismological Society of America*, **92**(5), 1878-1903. https://doi.org/10.1785/0120010156

17 Bradley BA, Bora SS, Lee RL, Manea EF, Gerstenberger MC, Stafford PJ, Atkinson GM, Weatherill G, Hutchinson J, de la Torre CA, Hulsey AM and Kaiser AE (2024). "The ground-motion characterisation model for the 2022 New Zealand national seismic hazard model". *Bulletin of the Seismological Society of America*, **114**(1), 329-349. https://doi.org/10.1785/0120230170

18 Abrahamson NA, Silva WJ and Kamai R (2014). "Summary of the ASK14 ground motion relation for active crustal regions". *Earthquake Spectra*, **30**(3), 1025-1055. https://doi.org/10.1193/070913EQS198M

19 Chiou BSJ and Youngs RR (2014). "Update of the Chiou and Youngs NGA model for the average horizontal component of peak ground motion and response spectra". *Earthquake Spectra*, **30**(3), 1117-1153. https://doi.org/10.1193/072813EQS219M

20 Francis TC, Sullivan TJ, Hulsey A and Elwood K (2025). "Recommendations for the shape of the design response spectrum in the New Zealand seismic loadings technical specification". *Bulletin of the New Zealand Society for Earthquake Engineering*, **58**(2). https://doi.org/10.5459/bnzsee.1692

21 Kaiser AE, Hill MP, de la Torre C, Bora S, Manea E, Wotherspoon L, Atkinson GM, Lee R, Bradley B, Hulsey A, Stolte A and Gerstenberger M (2024). "Overview of Site Effects and the Application of the 2022 New Zealand NSHM in the Wellington Basin, New Zealand". *Bulletin of the Seismological Society of America*, **114**(1): 399–421. https://doi.org/10.1785/0120230189

22 Wotherspoon LM, Kaiser AE, Stolte AC and Manea EF (2024). "Development of the site characterization database for the 2022 New Zealand National Seismic Hazard Model". *Seismological Research Letters*, **95**(1), 214-225. https://doi.org/10.1785/0220230219

23 Foster KM, Bradley BA, McGann CR and Wotherspoon, LM (2019). "A $V_{S30}$ map for New Zealand based on geologic and terrain proxy variables and field measurements". *Earthquake Spectra*, **35**(4): 1865-1897. https://doi.org/10.1193/121118EQS281M

24 Perrin ND, Heron DW, Kaiser AE and Van Houtte C (2015). "$V_{S30}$ and NZS 1170.5 site class maps of New Zealand". *2015 New Zealand Society for Earthquake Engineering Annual Technical Conference*, April 10-12, Rotorua, New Zealand, Paper No O-07, 8pp.

25 New Zealand Geotechnical Society/Ministry of Business and Employment (2021a). "*Earthquake Geotechnical Engineering Practice Module 3. Identification, Assessment and Mitigation of Liquefaction Hazards*". Rev 1. New Zealand Geotechnical Society/Ministry of Business and Employment, Wellington, NZ.

26 New Zealand Geotechnical Society/Ministry of Business and Employment (2021b). "*Earthquake Geotechnical Engineering Practice Module 4. Earthquake Resistant Foundation Design*". Rev 1. New Zealand Geotechnical Society/Ministry of Business and Employment, Wellington, NZ.

27 New Zealand Geotechnical Society/Ministry of Business and Employment (2024). "*Earthquake Geotechnical Engineering Practice Module 2. Geotechnical Investigations for Earthquake Engineering*". Rev 2 draft. New Zealand Geotechnical Society/Ministry of Business and Employment, Wellington, NZ.

28 Foti S, Hollender F, Garofalo F, Albarello D, Asten M, Bard PY, Comina C, Cornou C, Cox B, Di Giulio G, Forbriger T, Hayashi K, Lunedei E, Martin A, Mercerat D, Ohrnberger M, Poggi V, Renalier F, Sicilia D and Socco V (2018). "Guidelines for the good practice of surface wave analysis: a product of the InterPACIFIC project". *Bulletin of Earthquake Engineering*, **16**: 2367-2420. https://doi.org/10.1007/s10518-017-0206-7

29 Wentz R (2019). *Invasive Seismic Testing: A Summary of Methods and Good Practice*. Quake Centre Report, Christchurch, 72pp. https://resources.quakecentre.co.nz/invasive-seismic-testing-a-summary-of-methods-and-good-practice/

30 Wotherspoon LM, Wentz R, Cox BR and Stolte AC (2021). "Assessing the quality and uncertainty of in-situ seismic investigation methods". *2021 New Zealand Geotechnical Society Symposium*, March 24-26, Dunedin, New Zealand, 10pp. https://www.nzgs.org/libraries/assessing-the-quality-and-uncertainty-of-in-situ-seismic-investigation-methods/

31 Wotherspoon LM, Stolte AC and Wentz R (2023). Providing robust $V_{S30}$ estimates for seismic site classification in New Zealand, NZ Geomechanics News, Issue 105, July 2023. https://www.nzgs.org/libraries/providing-robust-vs30-estimates-for-seismic-site-classification-in-new-zealand/

32 NZGS (2022). *NZGS_200 Ground Investigations*, NZGS Specification, 124pp https://www.nzgs.org/libraries/nzgs-specifications/

33 Stolte AC and Cox BR (2020). "Towards consideration of epistemic uncertainty in shear-wave velocity measurements obtained via seismic cone penetration testing (SCPT)". *Canadian Geotechnical Journal*, **57**(1): 48-60. https://doi.org/10.1139/cgj-2018-0689

34 Seyhan E, Stewart JP, Ancheta TD, Darragh RB and Graves RW (2014). "NGA-West2 site database". *Earthquake Spectra*, **30**(3): 1007-1024. https://doi.org/10.1193/062913EQS180M

35 Teague D, Cox B, Bradley BA, and Wotherspoon LM (2018). "Development of Deep Shear Wave Velocity Profiles with Estimates of Uncertainty in the Complex Interbedded Geology of Christchurch, New Zealand". *Earthquake Spectra*, **34**(2): 639-672. https://doi.org/10.1193/041117EQS069M

36 Vantassel J, Cox B, Wotherspoon LM and Stolte AC (2018). "Mapping Depth to Bedrock, Shear Stiffness, and Fundamental Site Period at CentrePort, Wellington, Using Surface-Wave Methods: Implications for Local Seismic Site Amplification". *Bulletin of the Seismological Society of America*, **108**(3B): 1709-1721. https://doi.org/10.1785/0120170287

37 Boore DM (2004). "Estimating $\bar{V}_s(30)$ (or NEHRP site classes) from shallow velocity models (depths < 30 m)". *Bulletin of the Seismological Society of America*, **94**(2): 591-597. https://doi.org/10.1785/0120030105

38 Boore DM, Thompson EM and Cadet H (2011). "Regional correlations of $V_{S30}$ and velocities averaged over depths less than and greater than 30 meters". *Bulletin of the Seismological Society of America*, **101**(6): 3046-3059. https://doi.org/10.1785/0120110071

39 McGann CR, Bradley BA, Taylor ML, Wotherspoon LM and Cubrinovski M (2015). "Development of an empirical correlation for predicting shear wave velocity of Christchurch soils from cone penetration test data". *Soil Dynamics and Earthquake Engineering*, **75**: 66-75. https://doi.org/10.1016/j.soildyn.2015.03.023

40 McGann CR, Bradley BA and Jeong S (2018). "Empirical correlation for estimating shear-wave velocity from cone penetration test data for Banks Peninsula loess soils in Canterbury, New Zealand". *Journal of Geotechnical and Geoenvironmental Engineering*, **144**(9). https://doi.org/10.1061/(ASCE)GT.1943-5606.0001926

41 Andrus RD, Mohanan NP, Piratheepan P, Ellis BS and Holzer TL (2007). "Predicting shear-wave velocity from cone penetration resistance". 4th International Conference on Earthquake Geotechnical Engineering, June 25-28, Thessaloniki, Greece, Paper No 1454, 12pp.

42 Hegazy YA and Mayne PW (2006). "A global statistical correlation between shear wave velocity and cone penetration data". *GeoShanghai International Conference*, June 6-8, Shanghai, China, 6pp. https://doi.org/10.1061/40861(193)31

43 Robertson PK (2009). "Performance based earthquake design using the CPT". *International Conference on Performance-based design in Earthquake Geotechnical Engineering*, June 15-18, Tokyo, Japan, 21pp

44 Kwak DY, Brandenberg SJ, Mikami A and Stewart JP (2015). "Prediction equations for estimating shear-wave velocity from combined geotechnical and geomorphic indexes based on Japanese data set." *Bulletin of the Seismological Society of America*, **105**(4): 1919-1930. https://doi.org/10.1785/0120140326

45 Ohta Y and Goto N (1978). "Empirical shear wave velocity equations in terms of characteristic soil indexes". *Earthquake Engineering & Structural Dynamics*, **6**(2): 167-187. https://doi.org/10.1002/eqe.4290060205

46 Wair BR, DeJong JT and Shantz T (2012). *Guidelines for estimation of shear wave velocity profiles*. PEER 2012/08, Pacific Earthquake Engineering Research Center, University of California, Berkeley, CA, 95pp. https://peer.berkeley.edu/publications/2012-08

47 FEMA (Federal Emergency Management Agency) (2020) "NEHRP Recommended Seismic Provisions for New Buildings and Other Structures. (FEMA P-2082)", Washington DC.

48 Brandenberg SJ, Bellana N and Shantz T (2010). "Shear wave velocity as function of standard penetration test resistance and vertical effective stress at California bridge sites". *Soil Dynamics and Earthquake Engineering*, **30**(10): 1026-1035. https://doi.org/10.1016/j.soildyn.2010.04.014

49 Stirling MW, McVerry GH and Berryman KR (2002). "A new seismic hazard model for New Zealand". *Bulletin of the Seismological Society of America*, **92**(5): 1878-1903. https://doi.org/10.1785/0120110170

50 McVerry GH, Zhao JX, Abrahamson, NA and Somerville PG (2006). "New Zealand acceleration response spectrum attenuation relations for crustal and subduction zone earthquakes". *Bulletin of the New Zealand Society for Earthquake Engineering*, **39**(1): 1-58. https://doi.org/10.5459/bnzsee.39.1.1-58

## APPENDIX A: SITE CLASSIFICATION FOR ELASTIC SITE SPECTRA

*Table A1: Site classification criteria for elastic site spectra (reproduced from TS 1170.5)*

| Site Class | Site Class Criteria |
|---|---|
| I | Rock site with time-averaged shear-wave velocity in the top 30 m, $V_{s(30)} > 750$ m/s and the following additional characteristics:<br>a) The profile shall not contain material with a shear-wave velocity less than 600 m/s; and<br>b) There shall be no more than 3 m of soil or highly weathered rock between the bedrock and the ground surface. |
| II | Very stiff soil, very dense soil or soft rock with one of the following characteristics:<br>a) Time-averaged shear-wave velocity in the top 30 m, $450 < V_{s(30)} \leq 750$ m/s, and not underlain by materials with a shear-wave velocity less than 300 m/s; or<br>b) Time-averaged shear-wave velocity in the top 30 m, $V_{s(30)} > 750$ m/s, with more than 3 m of soil or highly weathered rock between the bedrock and the ground surface, or underlain by materials with a shear-wave velocity less than 600 m/s. |
| III | Stiff or dense soil with one of the following characteristics:<br>a) Time-averaged shear-wave velocity in the top 30 m, $300 < V_{s(30)} \leq 450$ m/s; or<br>b) Time-averaged shear-wave velocity in the top 30 m, $450 < V_{s(30)} \leq 750$ m/s, underlain by materials with a shear-wave velocity less than 300 m/s. |
| IV | Moderately stiff or medium dense soil with time-averaged shear-wave velocity in the top 30 m, $250 < V_{s(30)} \leq 300$ m/s. |
| V | Soft or loose soil with time-averaged shear-wave velocity in the top 30 m, $200 < V_{s(30)} \leq 250$ m/s, and the following soil characteristics from the ground surface to a depth of 20 m:<br>a) No more than 10 m of very soft soils with undrained shear strength less than 40 kPa; and<br>b) No more than 10 m of sandy soils or non-plastic silty soils with SPT $N_{60}$ values less than 6; and<br>c) No more than 10 m of sandy soils or non-plastic silty soils with $q_c$ values less than 2.5 MPa; and<br>d) No more than 10 m of clayey soils or plastic silty soils with $q_c$ values less than 1.0 MPa; and<br>e) No more than 10 m of soils with shear wave velocities of 150 m/s or less; and<br>f) No more than 10 m combined depth of soils with properties described in (a), (b), (c), or (d),above. |
| VI | Very soft or very loose soil with one of the following soil characteristics:<br>a) Time-averaged shear-wave velocity in the top 30 m, $150 \text{ m/s} < V_{s(30)} \leq 200$ m/s; or<br>b) Time-averaged shear-wave velocity in the top 30 m, $V_{s(30)} > 200$ m/s, with any of the following soil characteristics from the ground surface to a depth of 20 m:<br>i. More than 10 m of very soft soils with undrained shear strength less than 40 kPa; or<br>ii. More than 10 m of sandy soils or non-plastic silty soils with SPT $N_{60}$ values less than 6; or<br>iii. More than 10 m of sandy soils or non-plastic silty soils with $q_c$ values less than 2.5 MPa; or<br>iv. More than 10 m of clayey soils or plastic silty soils with $q_c$ values less than 1.0 MPa; or<br>v. More than 10 m of soils with shear wave velocities of 150 m/s or less; or<br>vi. More than 10 m combined depth of soils with properties described in (i), (ii), (iii), (iv), or (v) above. |
| VII | Sites with time-averaged shear-wave velocity in the top 30 m, $V_{s(30)} \leq 150$ m/s. See 3.1.3.2 of TS 1170.5. |

## APPENDIX B: EXAMPLES OF SITE CLASS DETERMINATION

### Method 1: Evaluation of $V_{s(30)}$ based on Direct Field Measurement of $V_s$ to at least 25 m Depth

*Example 1: Downhole $V_s$ measurement up to 25 m depth (Figure B1).*

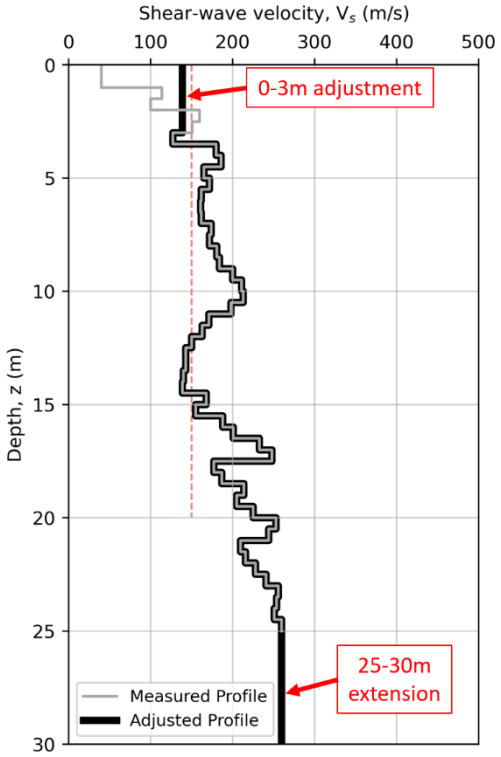


***Figure B1: $V_s$ profile obtained from direct downhole $V_s$ measurement to a depth of 25 m; the solid black line indicates the adjusted $V_s$ profile; the vertical dashed red line indicates $V_s$ = 150 m/s.***

Evaluation steps:

1. Less than 10 m of the $V_s$ profile is lower than 150 m/s over the top 20 m, hence Site Class VI and VII are provisionally ruled out based on cumulative thickness of soft soils criteria and $V_{s(30)}$-based classification can proceed.
2. Adjust $V_s$ from 0-3 m depth to adopt average $V_s$ between 2.5-3.5 m ($V_s$ = 139 m/s).
3. Extend last measured $V_s$ from 25 m to 30 m ($V_s$ = 260 m/s).
4. Calculate $V_{s(30)}$ of the adjusted profile (Eq. 3.6 of TS 1170.5):

$$V_{s(30)} = \frac{\sum_{i=1}^{n} t_i}{\sum_{i=1}^{n} \frac{t_i}{V_{si}}}$$
$$= 189 \text{ m/s}$$

5. Calculate lower and upper bound $V_{s(30)}$, $V_{s(30)\text{-}LB}$ and $V_{s(30)\text{-}UB}$, using 5% Method 1 uncertainty factor (Eq. C3.2 and Eq. C3.5 of TS 1170.5):

$$V_{s(30)-LB} = \frac{V_{s(30)}}{1.05}$$
$$= \frac{189}{1.05}$$
$$= 180 \text{ m/s}$$

$$V_{s(30)-UB} = 1.05 \times V_{s(30)}$$
$$= 1.05 \times 189$$
$$= 198 \text{ m/s}$$

6. Select appropriate site classes that span $V_{s(30)}$ = 180-198 m/s. The site is classified as Site Class VI (Table 3.1, TS 1170.5).

*Example 2: Multi-channel analysis of surface-wave (MASW) data up to 30 m depth (Figure B2). In this example, 10 profiles are used to serve as an illustration of how multiple profiles should be considered for site classification. However, to properly account for uncertainties in the inversion, including across different parameterisations of the inversion (e.g., different layering ratios), several hundreds of profiles or more may be required.*

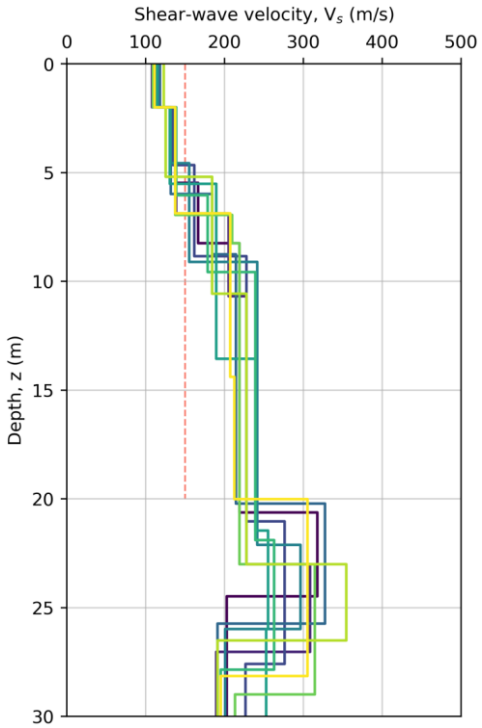


***Figure B2: 10 $V_s$ profiles obtained from multi-channel surface-wave analysis at one site; profiles with the 0-3 m depth adjustment are shown as solid lines and original measured profiles are shown as dashed grey lines (only visible between 0-3 m); the vertical dashed red line indicates $V_s$ = 150 m/s.***

Evaluation steps:

1. Select the 10 best-fit profiles from MASW inversions.
2. Less than 10 m of the $V_s$ profile is lower than 150 m/s over the top 20 m of every profile, hence Site Class VI and VII are provisionally ruled out based on cumulative thickness of soft soils criteria and $V_{s(30)}$-based classification can proceed.
3. Calculate $V_{s(30)}$ of each profile (Eq. 3.6 of TS 1170.5):

$$V_{s(30),j} = \frac{\sum_{i=1}^{n} t_i}{\sum_{i=1}^{n} \frac{t_i}{V_{si}}}$$

$$[V_{s(30),j}] = [V_{s(30),1}, V_{s(30),2}, \dots, V_{s(30),10}]$$
$$= [193, 194, \dots, 197] \text{ m/s}$$

4. Calculate average $V_{s(30)}$ across the 10 profiles:

$$V_{s(30)} = \text{average}([V_{s(30),j}])$$
$$= 196 \text{ m/s}$$

5. Calculate lower and upper bound $V_{s(30)}$, $V_{s(30)\text{-}LB}$ and $V_{s(30)\text{-}UB}$, using 5% Method 1 uncertainty factor (Eq. C3.2 and Eq. C3.5 of TS 1170.5):

$$V_{s(30)-\text{LB}} = \frac{V_{s(30)}}{1.05}$$
$$= \frac{196}{1.05}$$
$$= 187 \text{ m/s}$$
$$V_{s(30)-UB} = 1.05 \times V_{s(30)}$$
$$= 1.05 \times 196$$
$$= 206 \text{ m/s}$$

6. Select appropriate site classes that span $V_{s(30)}$ = 187-206 m/s. This site would require consideration of Site Class VI and Site Class V (i.e., multiple site classes) (Table 3.1, TS 1170.5).

**Method 2: Evaluation of $V_{s(30)}$ based on Direct Field Measurement of $V_s$ to at least 15 m Depth**

*Example 3: Downhole $V_s$ measurement up to 18.5 m depth (Figure B3).*

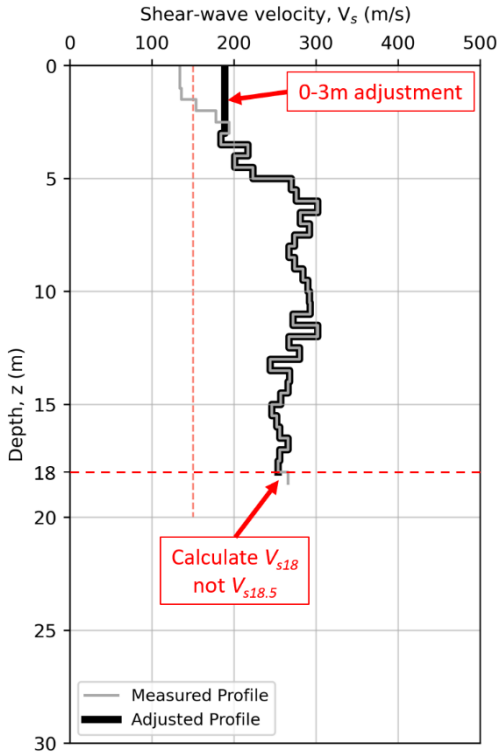


***Figure B3: $V_s$ profile obtained from downhole $V_s$ measurement at the site to a depth of 18.5 m; the solid black line indicates the adjusted $V_s$ profile; the vertical dashed red line indicates $V_s$ = 150 m/s.***

Evaluation steps:

1. Less than 10 m of the $V_s$ profile is lower than 150 m/s over the top 20 m, hence Site Class VI and VII are provisionally ruled out based on cumulative thickness of soft soils criteria and $V_{s(30)}$-based classification can proceed.
2. Adjust $V_s$ from 0-3 m depth to the adopt average $V_s$ between 2.5-3.5 m ($V_s$ = 189 m/s).
3. Calculate $V_{s18}$ based on the adjusted profile. 18 m is the whole number value of 18.5 m rounded down, as required for Boore (2004) $V_{sz}$-$V_{s(30)}$ correlation:

$$V_{s18} = \frac{\sum_{i=1}^{n} t_i}{\sum_{i=1}^{n} \frac{t_i}{V_{si}}} = 245 \text{ m/s}$$

4. Estimate $V_{s(30)}$ using $V_{s18}$ = 245 m/s in the Boore (2004) $V_{sz}$-$V_{s(30)}$ correlation (Eq. C3.13 of TS 1170.5). For $z$ = 18 m, the Boore (2004) coefficients are $a = 0.025$ and $b = 1.014$ (Table C3.4, TS 1170.5):

$$\begin{aligned} \log_{10} V_{s(30)} &= a + b \log_{10} V_{sz} \\ &= 0.025 + 1.014 \log_{10} V_{s18} \\ &= 0.025 + 1.014 \log_{10} 245 \\ V_{s(30)} &= 10^{0.025 + 1.014 \log_{10} 245} \\ &= 280 \text{ m/s} \end{aligned}$$

5. Calculate lower and upper bound $V_{s(30)}$, $V_{s(30)\text{-}LB}$ and $V_{s(30)\text{-}UB}$, with the Method 2 equations (Eq. C3.3 and Eq. C3.6 of TS 1170.5) and $z$ = 18 m (effectively 12% uncertainty factor corresponding to 18 m of measured $V_s$):

$$\begin{aligned} V_{s(30)-LB} &= \frac{V_{s(30)}}{1.15 - 0.01 \times (z - 15)} \\ &= \frac{280}{1.15 - 0.01 \times (18 - 15)} \\ &= 250 \text{ m/s} \end{aligned}$$

$$V_{s(30)-UB} = \{1.15 - 0.01 \times (z - 15)\} \times V_{s(30)}$$
$$= \{1.15 - 0.01 \times (18 - 15)\} \times 280$$
$$= 314 \text{ m/s}$$

6. Select appropriate site classes that span $V_{s(30)}$ = 250-314 m/s. This site would require consideration of Site Classes IV and III (i.e., multiple site classes) (Table 3.1, TS 1170.5). *Note: Site Class V was not considered as* $V_{s(30)-LB}$ = 250.1 m/s *was rounded to 250 m/s above.*

*Example 4: Partially measured $V_s$ profile to 21 m depth supplemented with CPT to 30 m with identified lower boundary of the soil layer that $V_s$ measurements terminate within (Figure B4). The profile comprises predominantly Holocene-aged soils, and the location is not in Christchurch.*

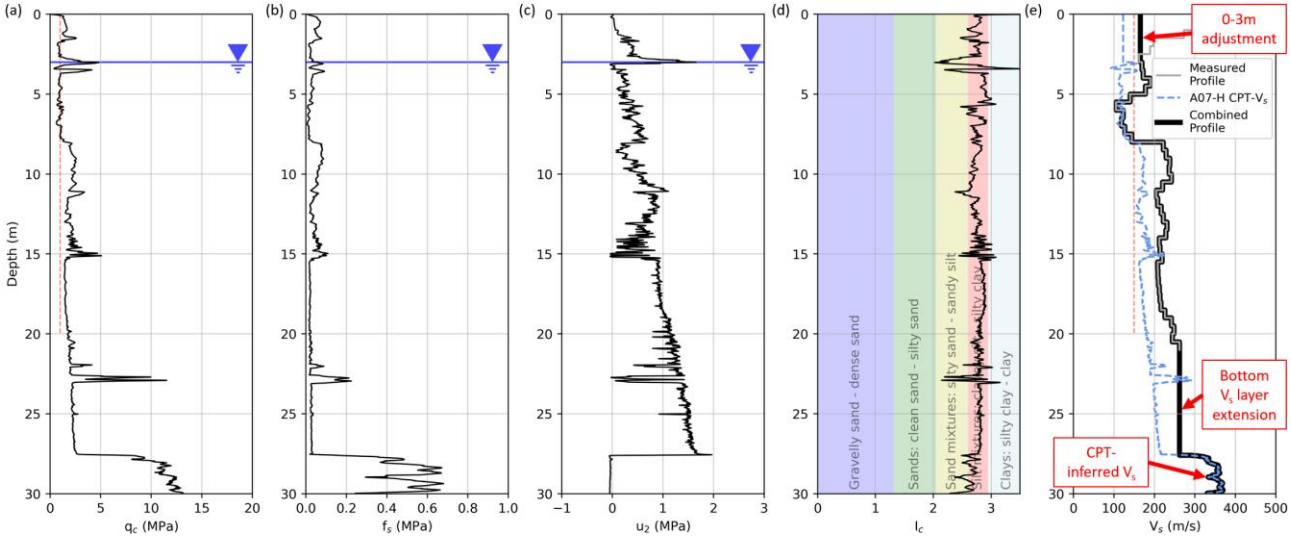


***Figure B4: Partially measured $V_s$ profile to 21 m depth supplemented with CPT-inferred $V_s$ to 30 m with identified lower boundary of the soil layer that $V_s$ measurements terminate within: (a) $q_c$; (b) $f_s$; (c) $u_2$; (d) $I_c$; and (e) $V_s$. The water table is located at 3.0 m depth. The vertical dashed red line in panel (a) indicates $q_c$ = 1.0 MPa and in panel (e) indicates $V_s$ = 150 m/s.***

Evaluation steps:

1. Less than 10 m of the $q_c$ profile is lower than 2.5 MPa for cohesionless soils and 1.0 MPa for cohesive soils over the top 20 m of the CPT, hence Site Class VI and VII are provisionally ruled out based on cumulative thickness of soft soils criteria and $V_{s(30)}$-based classification can proceed.
2. Adjust $V_s$ from 0-3 m depth to adopt the average $V_s$ between 2.5-3.5 m ($V_s$ = 166 m/s).
3. Identify bottom of soil layer that the measured $V_s$ terminates within in the CPT trace ($z$ = 27.6 m).
4. Extend last measured $V_s$ to identified bottom of the respective soil layer (i.e., the bottom of the layer of last measured $V_s$ terminates at $z$ = 27.6 m; $V_s$ = 262 m/s is extended to 27.6 m depth).
5. Calculate $V_s$ from CPT measurements using Andrus et al. (2007) Holocene CPT-$V_s$ correlation (Eq. C3.10 of TS 1170.5). For Holocene soils, SF = 0.92.

$$\ln V_s = \ln 2.62 + 0.395 \ln q_t + 0.912 \ln I_c + 0.124 \ln z + \ln SF$$

6. Append the CPT-inferred $V_s$ to the adjusted $V_s$ profile, from $z$ = 27.6 m to $z$ = 30 m.
7. Calculate $V_{s(30)}$ of the established combined profile (thick black line in Figure B4e):

$$V_{s(30)} = 209 \text{ m/s}$$

8. Calculate lower and upper bound $V_{s(30)}$, $V_{s(30)\text{-}LB}$ and $V_{s(30)\text{-}UB}$, with the Method 2 equations (Eq. C3.3 and Eq. C3.6 of TS 1170.5) and $z$ = 21 m (effectively 9% uncertainty factor corresponding to 21 m of measured $V_s$):

$$\begin{aligned} V_{s(30)-LB} &= \frac{V_{s(30)}}{1.15 - 0.01 \times (z - 15)} \\ &= \frac{209}{1.15 - 0.01 \times (21 - 15)} \\ &= 192 \text{ m/s} \end{aligned}$$

$$\begin{aligned} V_{s(30)-UB} &= \{1.15 - 0.01 \times (z - 15)\} \times V_{s(30)} \\ &= \{1.15 - 0.01 \times (21 - 15)\} \times 209 \\ &= 228 \text{ m/s} \end{aligned}$$

9. The combined depths over the profile where $q_c$ < 2.5 MPa for cohesionless soils, $q_c$ < 1.0 MPa for cohesive soils or $V_s$ < 150 m/s is less than 10 m over the top 20 m of the profile, hence Site Class VI based on cumulative thickness of soft soils criteria is ruled out and site classification can be based solely on $V_{s(30)}$.
10. Select appropriate site classes that span $V_{s(30)}$ = 192-228 m/s. This site would require consideration of Site Classes VI and V (i.e., multiple site classes) (Table 3.1, TS 1170.5).

**Method 3: Evaluation of $V_{s(30)}$ Primarily based on Inferred or Estimated $V_s$**

*Example 5: A site is located in Christchurch. Three CPTs with termination at 20 m (Figure B5a-e), 24 m (Figure B5f-j) and 25 m depth (Figure B5k-o), respectively.*

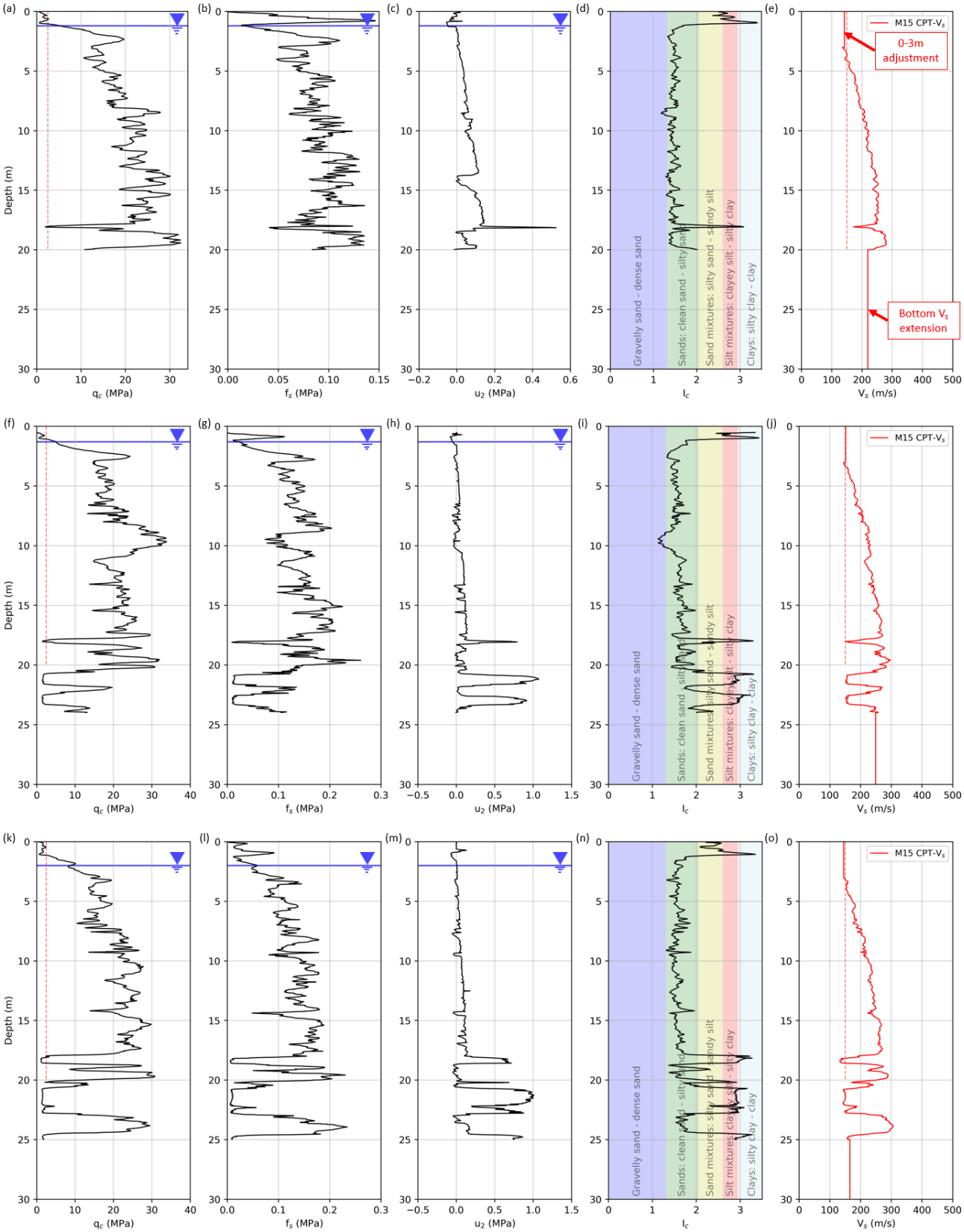


***Figure B5: CPT_1 profile with termination at 20 m depth: (a) $q_c$; (b) $f_s$; (c) $u_2$; (d) $I_c$; (e) $V_s$; CPT_2 profile with termination at 24 m depth: (f) $q_c$; (g) $f_s$; (h) $u_2$; (i) $I_c$; and (j) $V_s$; and CPT_3 profile with termination at 25 m depth: (k) $q_c$; (l) $f_s$; (m) $u_2$; (n) $I_c$; and (o) $V_s$. The water table is located at 1.2 m, 1.3 m and 2.0 m depths for CPT_1, CPT_2 and CPT_3, respectively. The vertical dashed red lines in panel (a), (f) and (k) indicate $q_c$ = 2.5 MPa, and in panels (e), (j) and (o) indicate $V_s$ = 150 m/s.***

Evaluation steps:

1. Less than 10 m of the $q_c$ profile is lower than 2.5 MPa for cohesionless soils and 1.0 MPa for cohesive soils over the top 20 m of the CPT, hence Site Class VI and VII are provisionally ruled out based on cumulative thickness of soft soils criteria and $V_{s(30)}$-based classification can proceed.
2. For each CPT, calculate $V_s$ down the depth of the CPT trace using the McGann et al. (2015) model (Eq. C3.8 of TS 1170.5).

$$\ln V_s = \ln 18.4 + 0.144 \ln q_c + 0.0832 \ln f_s + 0.278 \ln z$$

3. For each CPT, adjust $V_s$ from 0-3 m depth to adopt the average $V_s$ between 2.5-3.5 m ($V_s$ = 142 m/s for CPT_1, $V_s$ = 151 m/s for CPT_2 and $V_s$ = 145 m/s for CPT_3).
4. For each CPT, extend the bottom measured $V_s$ to 30 m depth ($V_s$ = 219 m/s for CPT_1, $V_s$ = 249 m/s for CPT_2 and $V_s$ = 165 m/s for CPT_3).
5. Calculate $V_{s(30)}$ of CPT_1 based on the adjusted profile:

$$V_{s(30),\text{CPT\_1}} = 203 \text{ m/s}$$

6. Calculate $V_{s(30)}$ of CPT_2 based on the adjusted profile:

$$V_{s(30),\text{CPT\_2}} = 211 \text{ m/s}$$

7. Calculate $V_{s(30)}$ of CPT_3 based on the adjusted profile:

$$V_{s(30),\text{CPT\_3}} = 191 \text{ m/s}$$

8. Calculate a weighted-average representative $V_{s(30)}$ of the site based on the three CPT-inferred $V_{s(30)}$. This should be weighted by the total investigation depth of each geotechnical test (e.g., CPT):

$$\begin{aligned} V_{s(30)} &= \frac{20 \times V_{s(30),\text{CPT\_1}} + 24 \times V_{s(30),\text{CPT\_2}} + 25 \times V_{s(30),\text{CPT\_3}}}{20 + 24 + 25} \\ &= \frac{20 \times 203 + 24 \times 211 + 25 \times 191}{20 + 24 + 25} \\ &= 201 \text{ m/s} \end{aligned}$$

9. Calculate lower and upper bound $V_{s(30)}$, $V_{s(30)\text{-}LB}$ and $V_{s(30)\text{-}UB}$, based on 30% Method 3 uncertainty factor (Eq. C3.4 and Eq. C3.7 of TS 1170.5):

$$\begin{aligned} V_{s(30)-LB} &= \frac{V_{s(30)}}{1.30} \\ &= \frac{201}{1.30} \\ &= 155 \text{ m/s} \end{aligned}$$

$$\begin{aligned} V_{s(30)-UB} &= 1.30 \times V_{s(30)} \\ &= 1.30 \times 201 \\ &= 261 \text{ m/s} \end{aligned}$$

10. The combined depths over the profile where $q_c$ < 2.5 MPa for cohesionless soils, $q_c$ < 1.0 MPa for cohesive soils or $V_s$ < 150 m/s is less than 10 m over the top 20 m of the profile, hence Site Class VI based on cumulative thickness of soft soils criteria is ruled out and site classification can be based solely on $V_{s(30)}$.
11. Select appropriate site classes that span $V_{s(30)}$ = 155-261 m/s. This site would require consideration of Site Classes VI, V and IV (i.e., multiple site classes) (Table 3.1, TS 1170.5).

*Example 6: A site located outside of Christchurch with predominantly Holocene-aged soils. Two CPTs to 20 m depth, but with refusal between 12-16 m where the default $V_s$=250 m/s is adopted (Figure B6).*

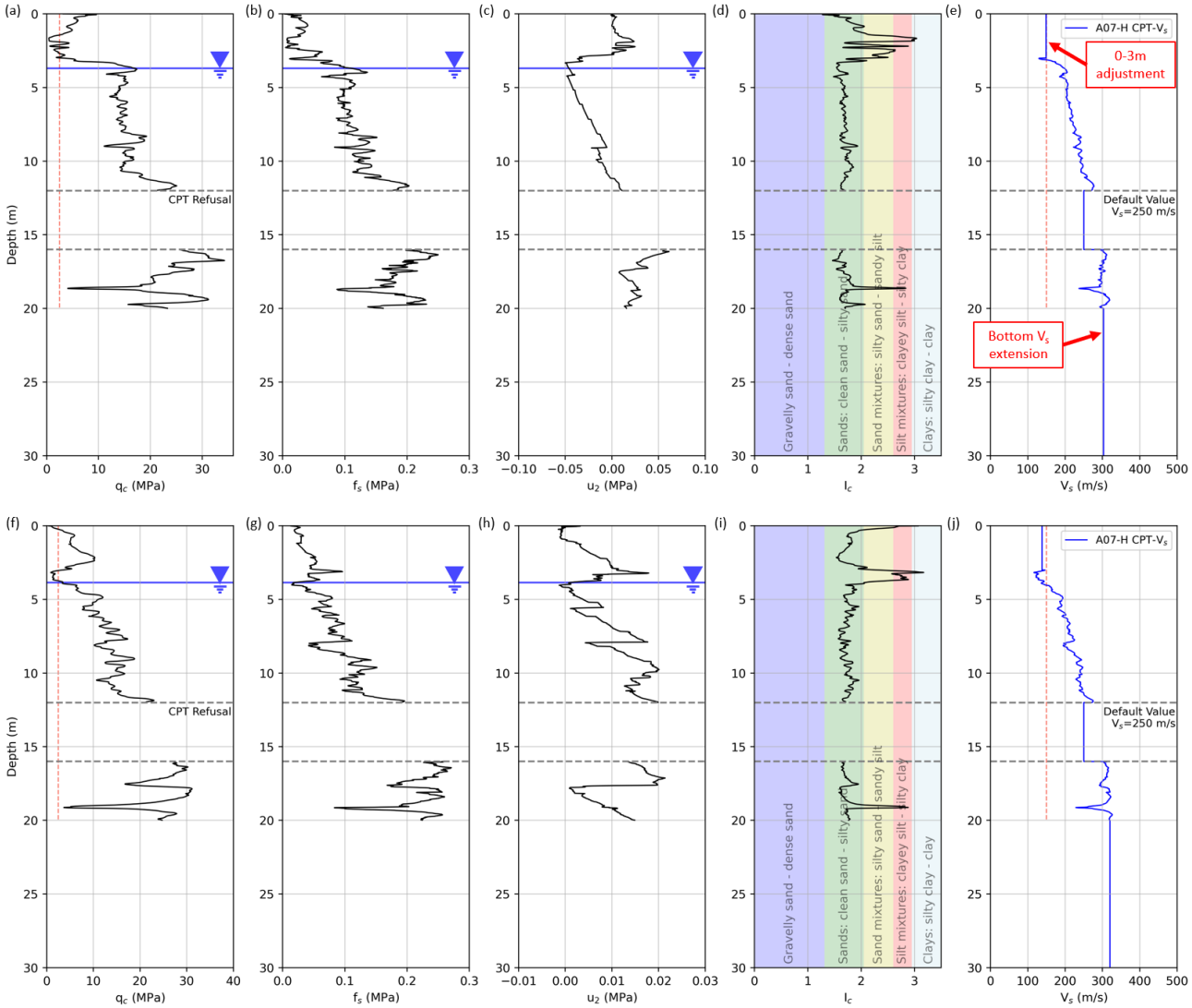


***Figure B6: CPT_4 profile with final depth at 20 m: (a) $q_c$; (b) $f_s$; (c) $u_2$; (d) $I_c$; (e) $V_s$; and CPT_5 profile with final depth at 20 m: (f) $q_c$; (g) $f_s$; (h) $u_2$; (i) $I_c$; and (j) $V_s$. Both CPT experienced refusal at 12 m depth resulting in pre-drilling between 12-16 m depth. Default $V_s$ = 250 m/s is adopted for the soil layer that caused CPT refusal. The water table is located at 3.7 m depth for CPT_4 and 3.85 m for CPT_5. The vertical dashed red lines in panel (a) and (f) indicate $q_c$ = 2.5 MPa, and in panels (e) and (j) indicate $V_s$ = 150 m/s.***

Evaluation steps:

1. Less than 10 m of the $q_c$ profile is lower than 2.5 MPa over the top 20 m of each CPT, hence Site Class VI and VII are provisionally ruled out based on cumulative thickness of soft soils criteria and $V_{s(30)}$-based classification can proceed.
2. For each CPT, calculate $V_s$ down the depth of the CPT trace using the Andrus et al. (2007) Holocene model (Eq. C3.10 of TS 1170.5). For Holocene soils, SF = 0.92.

$$\ln V_s = \ln 2.62 + 0.395 \ln q_t + 0.912 \ln I_c + 0.124 \ln z + \ln SF$$

3. For each CPT, adjust $V_s$ from 0-3 m depth to adopt average $V_s$ between 2.5-3.5 m ($V_s$ = 149 m/s for CPT_4 and $V_s$ = 138 m/s for CPT_5).
4. Adopt default $V_s$=250 m/s over the depth of CPT refusal (i.e., between 12-16 m) as cumulative depth of refusal is less than 5 m from ground surface to 20 m depth.
5. For each CPT, extend the bottom measured $V_s$ to 30 m depth ($V_s$ = 303 m/s for CPT_4 and $V_s$ = 320 m/s for CPT_5).
6. Calculate $V_{s(30)}$ of CPT_4 based on the adjusted profile:

$$V_{s(30),\text{CPT\_4}} = 243 \text{ m/s}$$

7. Calculate $V_{s(30)}$ of CPT_5 based on the adjusted profile:

$$V_{s(30),\text{CPT\_5}} = 236 \text{ m/s}$$

8. Calculate a weighted-average representative $V_{s(30)}$ of the site. Since the two CPT have the same final depth of investigation (20 m), the simple arithmetic average can be used (and is equivalent to the weighted average):

$$V_{s(30)} = \frac{243 + 236}{2}$$
$$= 240 \text{ m/s}$$

9. Calculate lower and upper bound $V_{s(30)}$, $V_{s(30)\text{-}LB}$ and $V_{s(30)\text{-}UB}$, based on 30% Method 3 uncertainty factor (Eq. C3.4 and Eq. C3.7 of TS 1170.5):

$$V_{s(30)-LB} = \frac{V_{s(30)}}{1.30}$$
$$= \frac{240}{1.30}$$
$$= 185 \text{ m/s}$$

$$V_{s(30)-UB} = 1.30 \times V_{s(30)}$$
$$= 1.30 \times 240$$
$$= 312 \text{ m/s}$$

10. The combined depths over the profile where $q_c$ < 2.5 MPa or $V_s$ < 150 m/s is less than 10 m over the top 20 m of the profile, hence Site Class VI based on cumulative thickness of soft soils criteria is ruled out and site classification can be based solely on $V_{s(30)}$.
11. Select appropriate site classes that span $V_{s(30)}$ = 185-312 m/s. This site would require consideration of Site Classes VI, V, IV and III (i.e., multiple site classes) (Table 3.1, TS 1170.5).

*Example 7: A site located outside of Christchurch with predominantly Pleistocene-aged soils. Two CPTs to 20 m; authoritative geologic model suggests $V_s$ = 250-350 m/s below 20 m depth (Figure B7).*

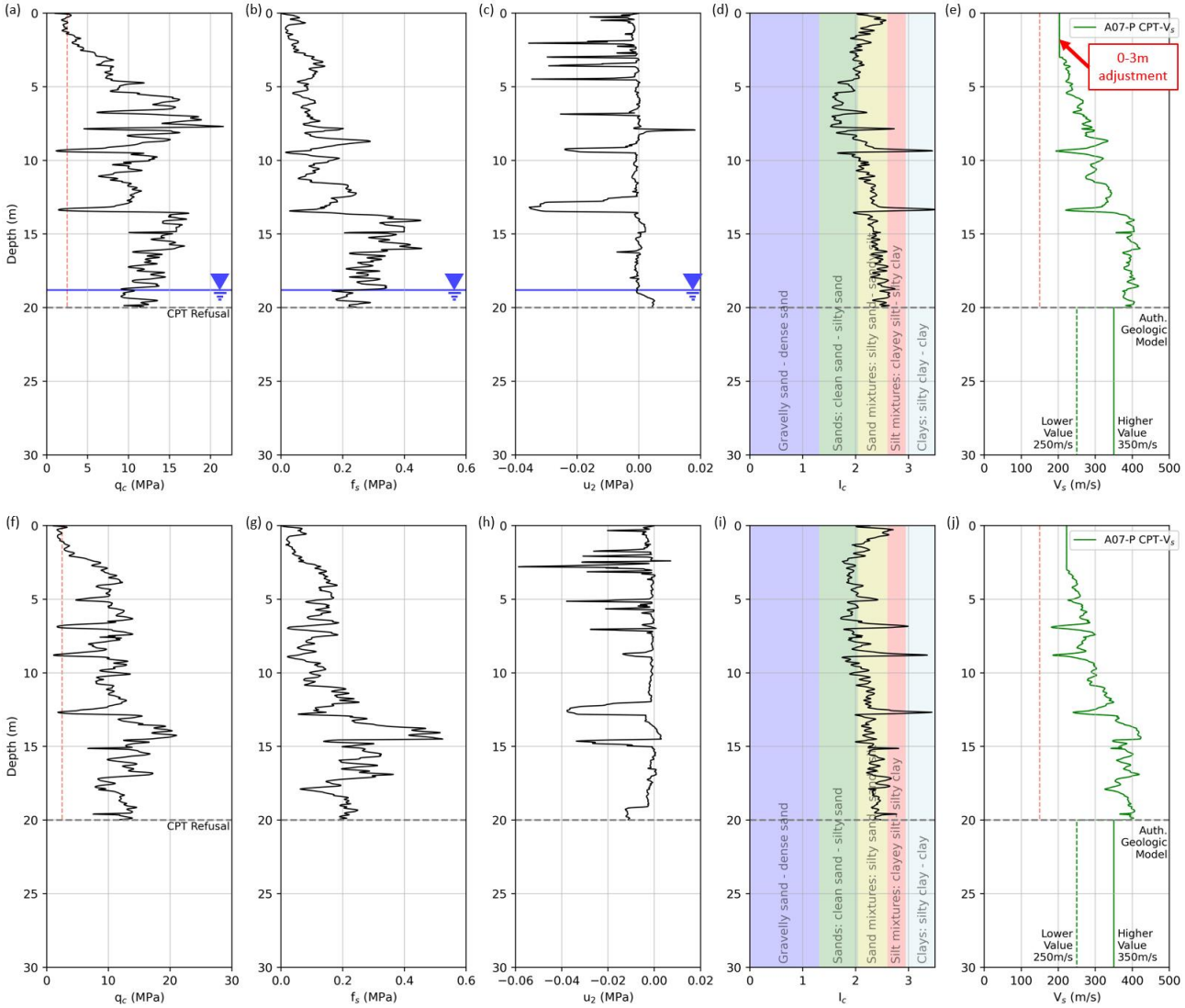


***Figure B7: CPT_6 profile with final depth at 20 m due to refusal: (a) $q_c$; (b) $f_s$; (c) $u_2$; (d) $I_c$; (e) $V_s$; and CPT_7 profile with final depth at 20 m due to refusal: (f) $q_c$; (g) $f_s$; (h) $u_2$; (i) $I_c$; and (j) $V_s$. Both CPT are supplemented with data from an authoritative geologic model between 20-30 m depth. The authoritative geologic model suggests $V_s$ between 250-350 m/s for depths between 20 m and 30 m. The water table is located at 18.8 m depth for CPT_6 and was not encountered within the depth of investigation for CPT_7. The vertical dashed red lines in panel (a) and (f) indicate $q_c$ = 2.5 MPa, and in panels (e) and (j) indicate $V_s$ = 150 m/s.***

Evaluation steps:

1. Less than 10 m of the $q_c$ profile is lower than 2.5 MPa over the top 20 m of each CPT, hence Site Class VI and VII are provisionally ruled out based on cumulative thickness of soft soils criteria and $V_{s(30)}$-based classification can proceed.
2. For each CPT, calculate $V_s$ down the depth of the CPT trace using the of Andrus et al. (2007) Pleistocene model (Eq. C3.10 of TS 1170.5). For Pleistocene soils, SF = 1.12.

$$\ln V_s = \ln 2.62 + 0.395 \ln q_t + 0.912 \ln I_c + 0.124 \ln z + \ln SF$$

3. For each CPT, adjust $V_s$ from 0-3 m depth to adopt the average $V_s$ between 2.5-3.5 m ($V_s$ = 204 m/s for CPT_6 and $V_s$ = 223 m/s for CPT_7).
4. Adopt the authoritative geologic model below 20 m.
5. Calculate $V_{s(30)}$ of the combined $V_s$ profile of CPT_6 using the lower $V_s$=250 m/s for the authoritative geologic model:

$$V_{s(30),\text{CPT\_6L}} = 272 \text{ m/s}$$

6. Calculate $V_{s(30)}$ of the combined $V_s$ profile of CPT_6 using the higher $V_s$=350 m/s for the authoritative geologic model:

$$V_{s(30),\text{CPT\_6U}} = 303 \text{ m/s}$$

7. Calculate $V_{s(30)}$ of the combined $V_s$ profile of CPT_7 using the lower $V_s$=250 m/s for the authoritative geologic model:

$$V_{s(30),\text{CPT\_7L}} = 276 \text{ m/s}$$

8. Calculate $V_{s(30)}$ of the combined $V_s$ profile of CPT_7 using the higher $V_s$=350 m/s for the authoritative geologic model:

$$V_{s(30),\text{CPT\_7U}} = 308 \text{ m/s}$$

9. Calculate lower bound $V_{s(30)\text{-}LB}$ using the minimum $V_{s(30)}$ across the two CPT with the lower $V_s$ for the authoritative geologic model based on 30% Method 3 uncertainty factor (Eq. C3.4 of TS 1170.5):

$$\begin{aligned} V_{s(30)-LB} &= \frac{\min\left[V_{s(30),\text{CPT\_6L}}, V_{s(30),\text{CPT\_7L}}\right]}{1.30} \\ &= \frac{\min[272, 276]}{1.30} \\ &= \frac{272}{1.30} \\ &= 209 \text{ m/s} \end{aligned}$$

10. Calculate upper bound $V_{s(30)\text{-}UB}$ using the maximum $V_{s(30)}$ across the two CPT with the higher $V_s$ for the authoritative geologic model based on 30% Method 3 uncertainty factor (Eq. C3.7 of TS 1170.5):

$$\begin{aligned} V_{s(30)-UB} &= 1.30 \times \max\left[V_{s(30),\text{CPT\_6U}}, V_{s(30),\text{CPT\_7U}}\right] \\ &= 1.30 \times \max[303, 308] \\ &= 1.30 \times 308 \\ &= 400 \text{ m/s} \end{aligned}$$

11. The combined depths over the profile where $q_c$ < 2.5 MPa or $V_s$ < 150 m/s is less than 10 m over the top 20 m of the profile, hence Site Class VI based on cumulative thickness of soft soils criteria is ruled out and site classification can be based solely on $V_{s(30)}$.
12. Select appropriate site classes that span $V_{s(30)}$ = 209-400 m/s. This site would require consideration of Site Classes V, IV and III (i.e., multiple site classes) (Table 3.1, TS 1170.5).

*Example 8: Borehole with SPT measurements to 29 m depth illustrating SPT-$V_s$ correlations for a soil profile with gravels, sands and silts (Figure B8).*

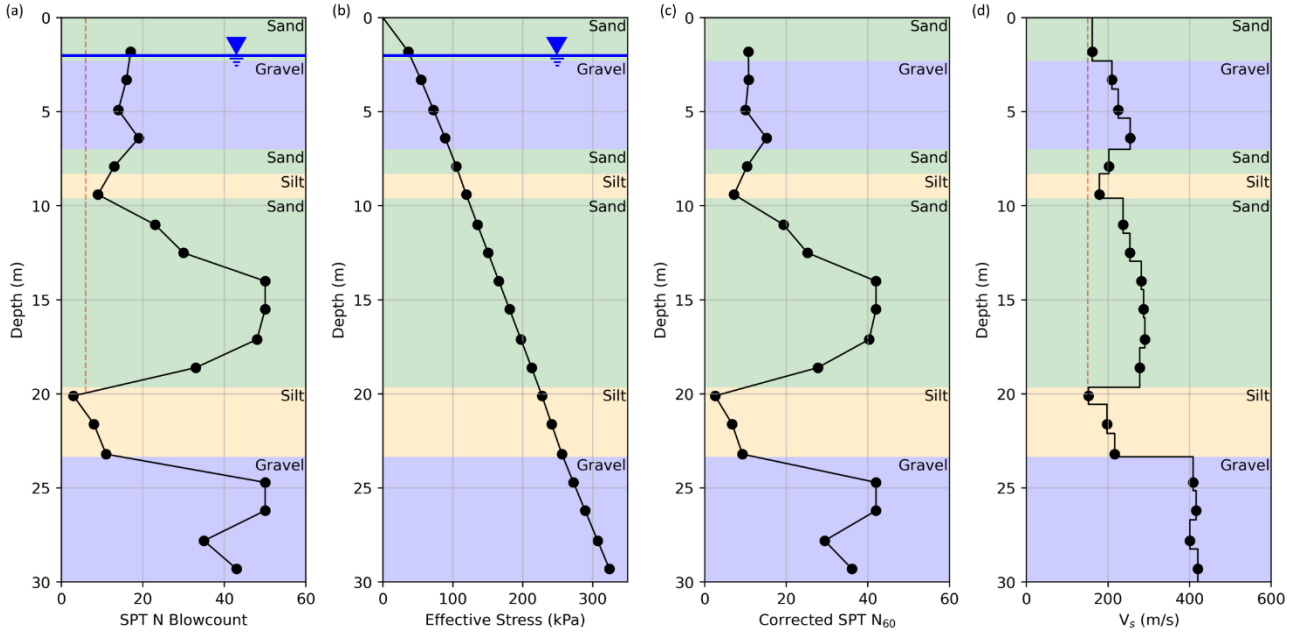


***Figure B8: SPT profile with measurements to 29 m depth including gravels, sands and silts: (a) SPT N; (b) effective stress; (c) SPT $N_{60}$; and (d) $V_s$. The depth corresponding to each SPT N value and subsequently calculated parameters is between the second and third driven increments (the effective depth of the values that N comprises). The water table is located at 2.0 m depth. The vertical dashed red line in panel (a) indicates N = 6 and in panel (d) indicates $V_s$ = 150 m/s.***

Evaluation steps:

1. Less than 10 m of the SPT *N* profile is lower than 6 over the top 20 m of the SPT, hence Site Class VI and VII are provisionally ruled out based on cumulative thickness of soft soils criteria and $V_{s(30)}$-based classification can proceed.
2. Calculate $V_s$ at depths of SPT measurements using the appropriate formulation of Kwak et al. (2015) (Eq. C3.11 in TS 1170.5) for each soil type (regression coefficients $\beta$ from Table C3.2, TS 1170.5). The $V_s$ calculation requires calculation of intermediate soil profile parameters (effective stress $\sigma'_v$, for example based on assumed typical unit weights, and $N_{60}$).

$$\ln V_s = \beta_0 + \beta_1 \ln N_{60} + \beta_2 \ln \sigma'_v$$

3. Determine boundary depths for each SPT-inferred $V_s$ value adhering to soil layer boundaries established from the borehole data or using mid-distance between two SPT measurements within the same layer.
4. Calculate $V_{s(30)}$ of the inferred $V_s$ profile:

$$V_{s(30)} = 247 \text{ m/s}$$

5. Calculate lower and upper bound $V_{s(30)}$, $V_{s(30)\text{-}LB}$ and $V_{s(30)\text{-}UB}$, using 30% Method 3 uncertainty factor (Eq. C3.4 and C3.7 of TS 1170.5):

$$\begin{aligned} V_{s(30)-LB} &= \frac{V_{s(30)}}{1.30} \\ &= \frac{247}{1.30} \\ &= 190 \text{ m/s} \end{aligned}$$

$$\begin{aligned} V_{s(30)-UB} &= 1.30 \times V_{s(30)} \\ &= 1.30 \times 247 \\ &= 321 \text{ m/s} \end{aligned}$$

6. The combined depths over the profile where SPT $N < 6$ or $V_s < 150$ m/s is less than 10 m over the top 20 m of the profile, hence Site Class VI based on cumulative thickness of soft soils criteria is ruled out and site classification can be based solely on $V_{s(30)}$.
7. Select appropriate site classes that span $V_{s(30)}$ = 190-321 m/s. This site would require consideration of Site Classes VI, V, IV and III (i.e., multiple site classes) (Table 3.1, TS 1170.5).